A Tool Kit for Spectral Profile Analysis of Tokamak Edge Plasmas

R. C. Isler

March 17, 2011

Maslow's Maxim

- " To the man who only has a hammer in the toolkit, every problem looks like a nail."

Spectroscopic applications for edge plasmas

- Ion temperatures and parallel flows
- Static electric fields (hydrogen and helium)
- Dynamic electric fields
- Impurity release mechanisms and influxes

Russell-Saunders (L-S) Coupling

States of low-Z ions are characterized by quantum numbers S, L, J and m_J.

S=spin ang. mom. L=orbital ang. mom. J=total ang mom.
m_J=projection of J along z-axis.

$|L-S| \leq J \leq L+S \qquad -J \leq m_J \leq J$

Spectroscopic notation: S-state, L=0
P-state, L=1
D-state, L=2

S (spin) = 1/2 → fine structure doublets
1 → triplets

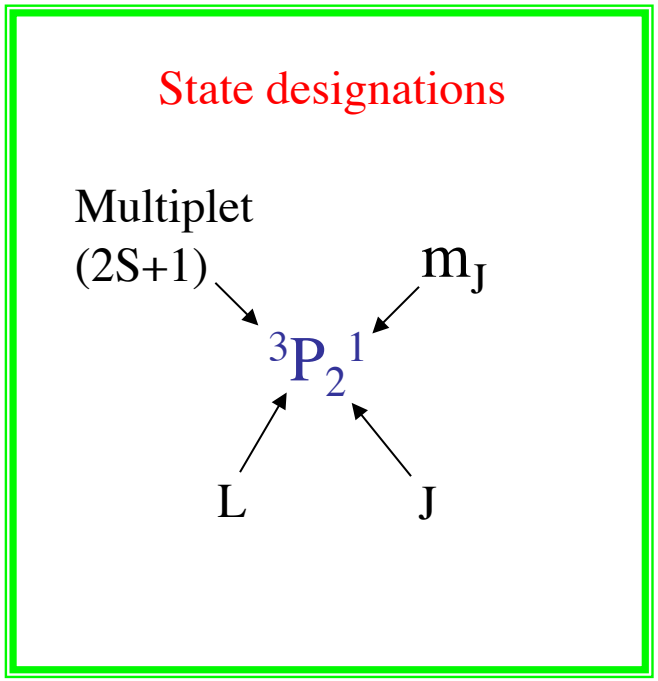

Each J-state has (2J+1) magnetic sublevels with $-J \leq m_J \leq J$.
These split into distinct energy levels in a magnetic field.

A He I Grotrian Diagram

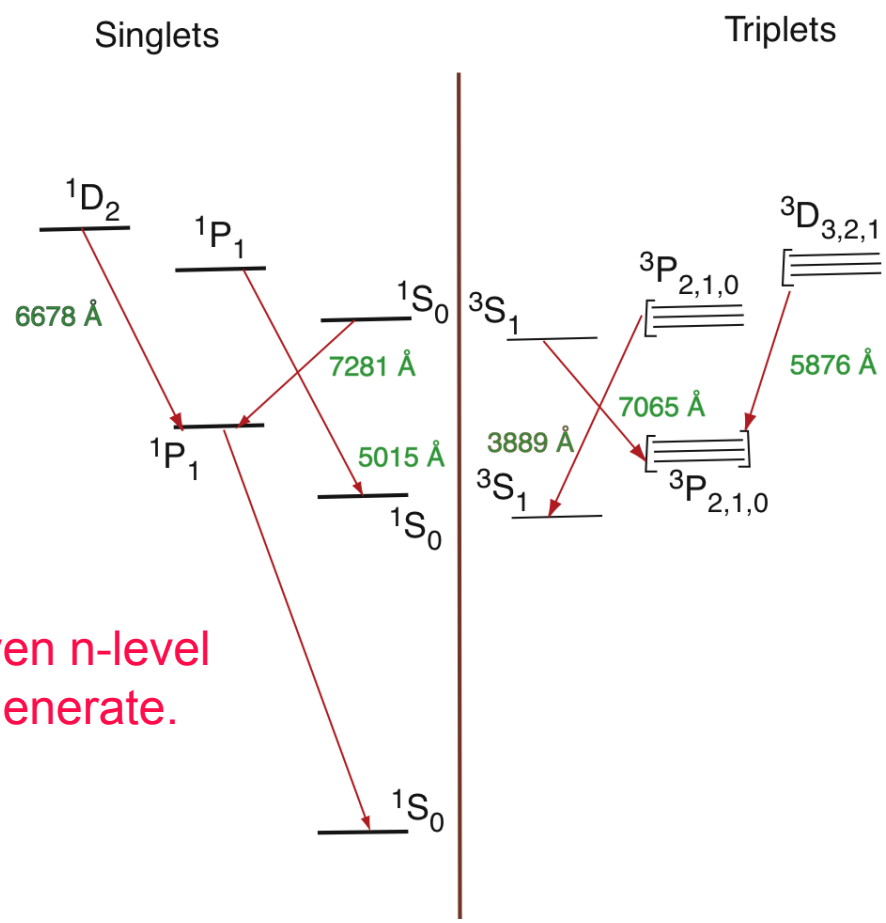

The L-states for a given n-level of helium are not degenerate.

Generating theoretical multiplet profiles requires two steps:

1. Calculating energy level splittings in external fields

2. Calculating the transition intensities between the eigenstates

We must first define a coordinate system

The Hamiltonian for Zeeman and Stark Effects

$$W + \Delta W = \left\langle \gamma' S L' J' m_j' \middle| H^0 + H' \middle| \gamma S L J m_j \right\rangle$$

S = spin quantum number
L = orbital quantum number
J = total angular momentum number
m_j = magnetic quantum number

$$H' = \zeta \vec{L} \bullet \vec{S} + \mu_b \vec{B} \bullet (\vec{L} + 2\vec{S}) + e\vec{E} \bullet \vec{r} \qquad \vec{B} = B_z \vec{\varepsilon}_z$$

Spin-orbit interaction

Zeeman Effect

Stark effect (observable only in hydrogen and helium)

Note: all operators are scalar products

An example of the Zeeman/Paschen-Bach effect

At low fields, the Zeeman effect is a small perturbation on the spin-orbit coupling. At high fields, the reverse is true. The eigenvalues and eigenvectors for arbitrary magnetic fields are found by diagonalizing the interaction matrix.

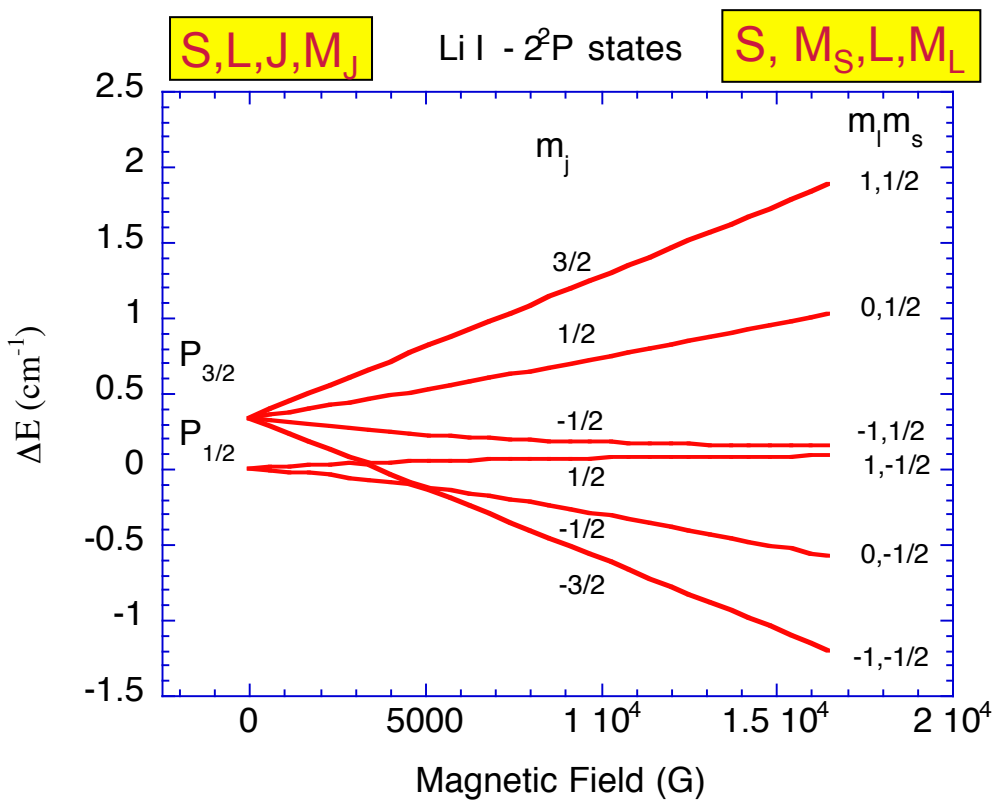

Matrix entries for the fine-structure plus Zeeman effect for a ^{3}P state

- Fine structure+Zeeman effect
- Zeeman effect

Off-diagonal elements occur only for $\Delta m_J=0$ and $\Delta J=\pm 1$.

	P_0^0	P_1^{-1}	P_1^0	P_1^1	P_2^{-2}	P_2^{-1}	P_2^0	P_2^1	P_2^2
P_0^0	●	0	●	0	0	0	0	0	0
P_1^{-1}	0	●	0	0	0	●	0	0	0
P_1^0	●	0	●	0	0	0	●	0	0
P_1^1	0	0	0	●	0	0	0	●	0
P_2^{-2}	0	0	0	0	●	0	0	0	0
P_2^{-1}	0	●	0	0	0	●	0	0	0
P_2^0	0	0	●	0	0	0	●	0	0
P_2^1	0	0	0	●	0	0	0	●	0
P_2^2	0	0	0	0	0	0	0	0	●

An example of Zeeman splitting in a tokamak environment

From ROTT6 Code

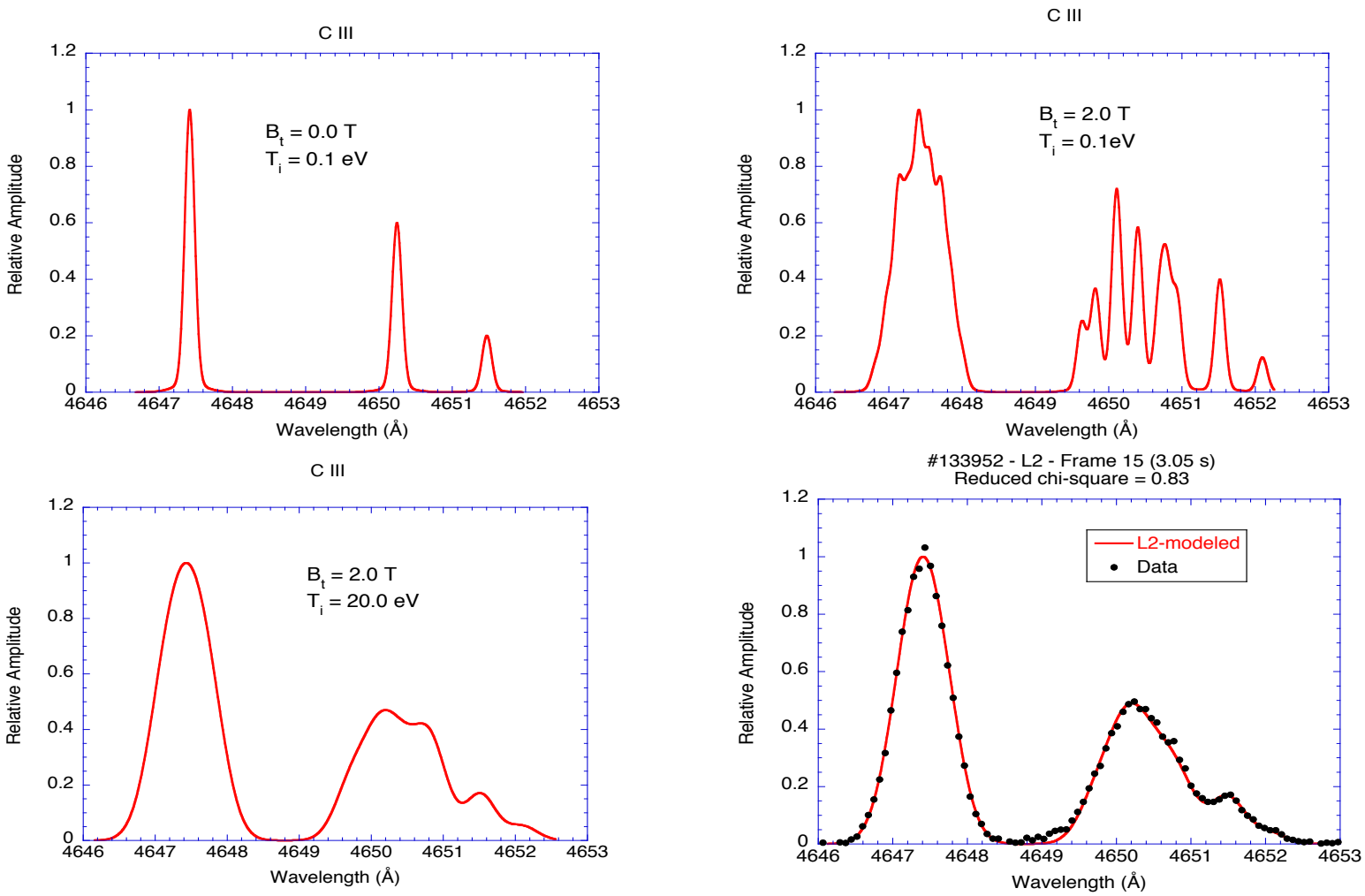

Zeeman Multiplet Spectra

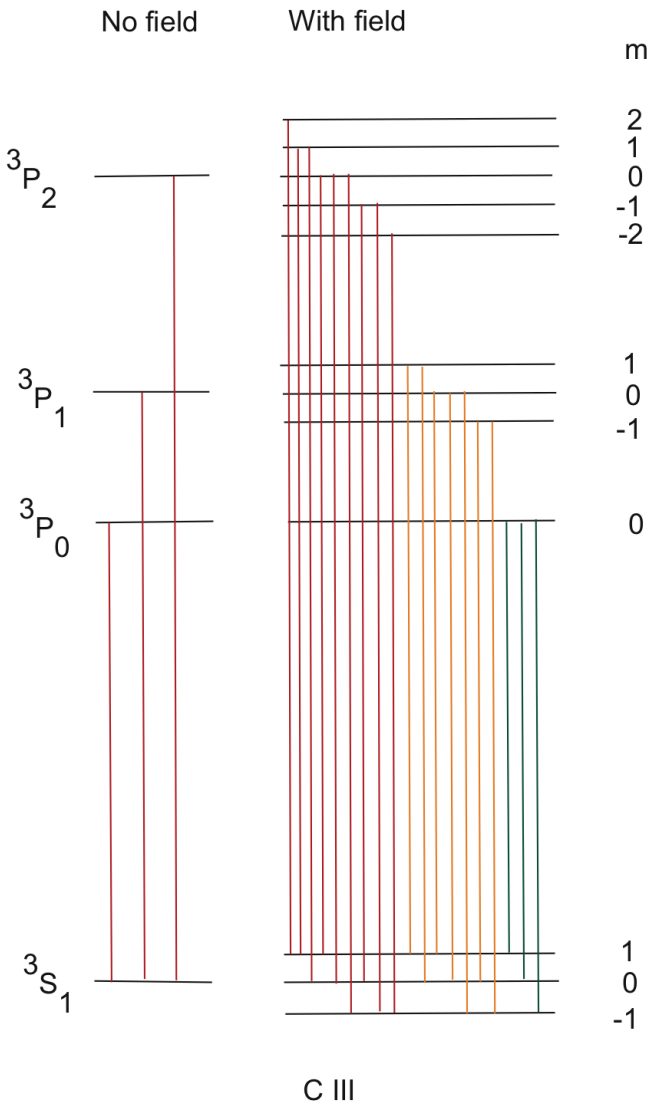

Once the eigenvalues (energy levels) and eigenfunctions have been calculated for the upper and lower levels of a multiplet, the transition intensities can be computed.

States with the same m-values are coupled. E.g.,

$$\Psi = \alpha P_0^0 + \beta P_1^0 + \eta P_2^0$$

Where α, β, η are the coefficients obtained from diagonalizing the interaction matrix.

Selection rules

$$\Delta J = 0, \pm 1 \quad but\ not\ J = 0\ to\ J' = 0$$
$$\Delta L = \pm 1$$
$$\Delta S = 0$$
$$\Delta M = 0, \pm 1$$

Δm = 0 transitions are linearly polarized parallel to B.
Δm = ±1 transitions are circularly polarized perpendicular to B.

Transition probabilities

The intensity of a spectral line in static field is given by

$$I \propto (\Psi \,|\, \vec{\varepsilon} \bullet \vec{r} \,|\, \Phi)(\Phi \,|\, \vec{\varepsilon} \bullet \vec{r} \,|\, \Psi)$$

Electric dipole

Where ε is a unit vector in the direction of the electric field of the radiation and r is the radial coordinate of the atom.

$$\vec{\varepsilon} \bullet \vec{r} = \varepsilon_x r_x + \varepsilon_y r_y + \varepsilon_z r_z$$

Spherical tensor notation:

$$\begin{cases} \vec{\varepsilon} \bullet \vec{r} = \sum_{q=-1}^{1} (-1)^q \varepsilon_q^1 r_{-q}^1 \\ r_{\pm 1} = \mp \frac{1}{\sqrt{2}} (x \pm iy); \quad r_0 = z \\ \varepsilon_{\pm 1} = \mp \frac{1}{\sqrt{2}} (\varepsilon_x \pm i\varepsilon_y); \quad \varepsilon_0 = \varepsilon_z \end{cases}$$

Calculation of Matrix Elements Only Requires Evaluation of Certain Algebraic Expressions

The Wigner-Eckart theorem:

$$-\varepsilon_{-q}(\gamma' S L' J' M' | r_q^{(1)}) | \gamma S L J M) = -\varepsilon_{-q}(-1)^{J'-M'} \begin{pmatrix} J' & 1 & J \\ -M' & q & M \end{pmatrix} (\gamma' S L' J' \| \mathbf{r}^{(1)} \| \gamma S L J)$$

3J symbol

Reduced matrix element

$$(\gamma' S L' J' \| \mathbf{r}^{(1)} \| \gamma S L J) = (-1)^{S+L+J'+1} [(2J+1)(2J'+1)]^{1/2} \begin{Bmatrix} L' & J' & S \\ J & L & 1 \end{Bmatrix} (\gamma' L' \| \mathbf{r}^{(1)} \| \gamma L)$$

6J symbol

For radiation

$$(\gamma' L' \| \mathbf{r}^{(1)} \| \gamma L)^2 = (2L'+1) A_{L'L}$$

Transition Probability

For the Stark effect

$$(\gamma' L' \| \mathbf{r}^{(1)} \| \gamma L) = \pm L_>^{1/2} \bullet \frac{3}{2} n (n^2 - L_>^2)^{1/2}$$

From Bethe and Saltpeter

Viewing Geometry

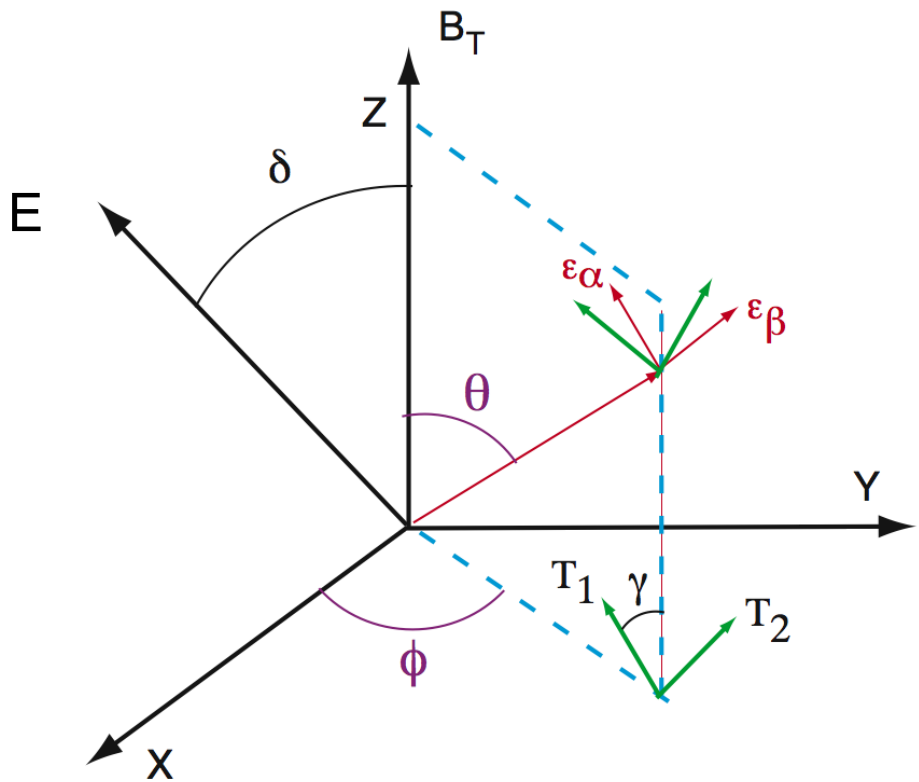

$$\varepsilon_z = \varepsilon_\alpha \sin\theta$$

$$\varepsilon_x = -\varepsilon_\beta \sin\phi - \varepsilon_\alpha \cos\theta \cos\phi$$

$$\varepsilon_y = \varepsilon_\beta \cos\phi - \varepsilon_\alpha \cos\theta \sin\phi$$

$$\varepsilon_\alpha = T_1 \cos\gamma + T_2 \sin\gamma$$

$$\varepsilon_\beta = T_1 \sin\gamma - T_2 \cos\gamma$$

Polarization

$$I \propto (\Psi \,|\, \vec{\varepsilon} \bullet \vec{r} \,|\, \Phi)(\Phi \,|\, \vec{\varepsilon} \bullet \vec{r} \,|\, \Psi) = \varepsilon^{+}\varepsilon^{-}(\Psi \,|\, r_{-1}^{(1)} \,|\, \Phi)(\Phi \,|\, r_{1}^{(1)} \,|\, \Psi)$$

$$I \propto \frac{1}{2}(\varepsilon_x^2 + \varepsilon_y^2)(\Psi \,|\, r_{-1}^{(1)} \,|\, \Phi)(\Phi \,|\, r_{1}^{(1)} \,|\, \Psi)$$

σ-transitions

$$I \propto \frac{1}{2}(1 + \cos^2\theta)(\Psi \,|\, r_{-1}^{(1)} \,|\, \Phi)(\Phi \,|\, r_{1}^{(1)} \,|\, \Psi)$$

The total emission is isotropic and unpolarized if all magnetic substates are equally populated.

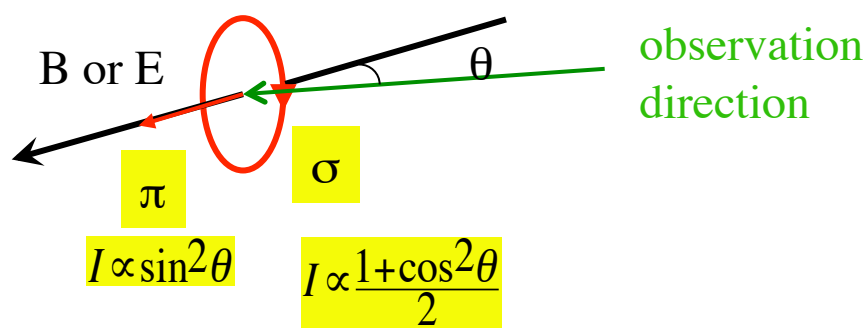

π transitions are not observed when viewing along a field.

σ transitions appear polarized perpendicular to the field when viewed perpendicular to the field

Quasi-tangential views in DIII-D (old)

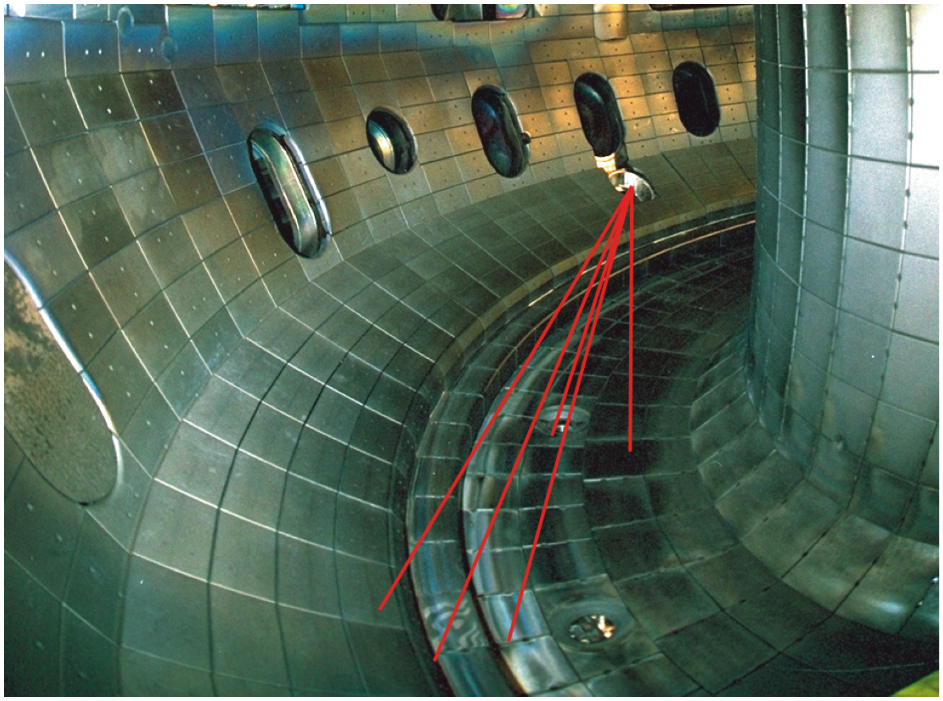

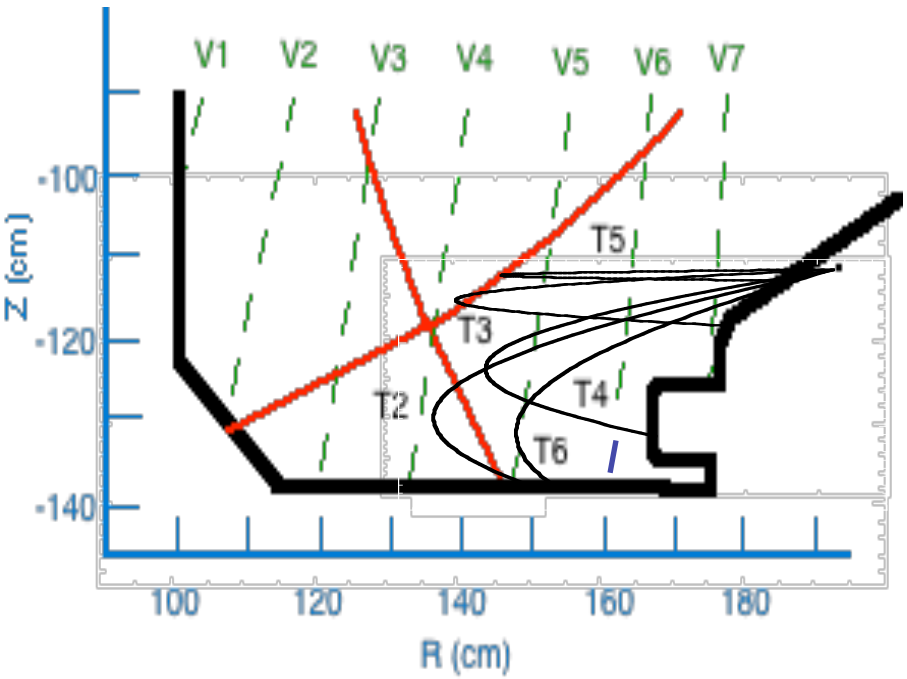

The projections of the quasi-tangential views in toroidal plane are hyperbolic segments.

Schematic of Current, Field,and Tangential Sight line Directions (grad-B drift downward)

Top View

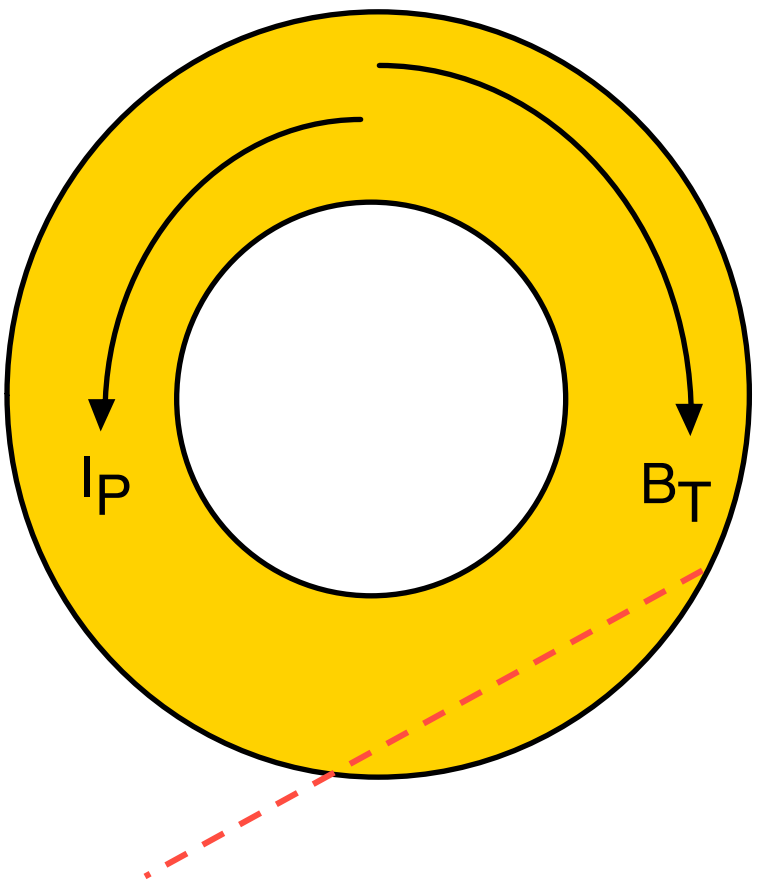

Sight line

Outer Leg

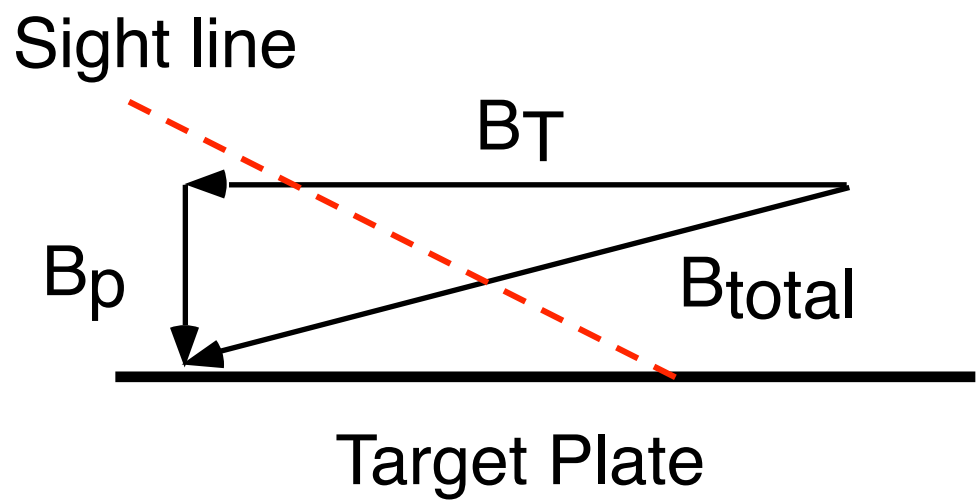

- In normal operation, spectral lines from ions flowing toward the target in the outer leg are blue-shifted

C II line profiles from the MDS spectrometer system

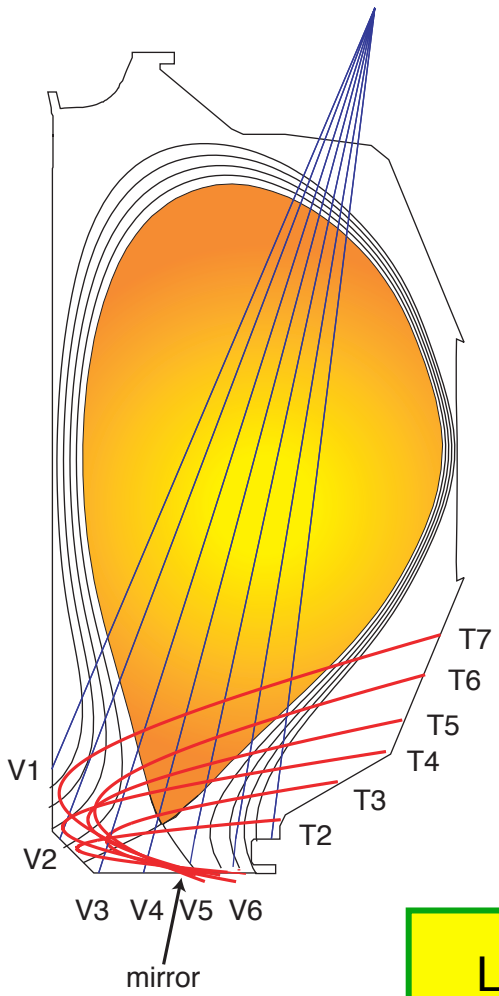

Vertical views provide references for measuring parallel flows

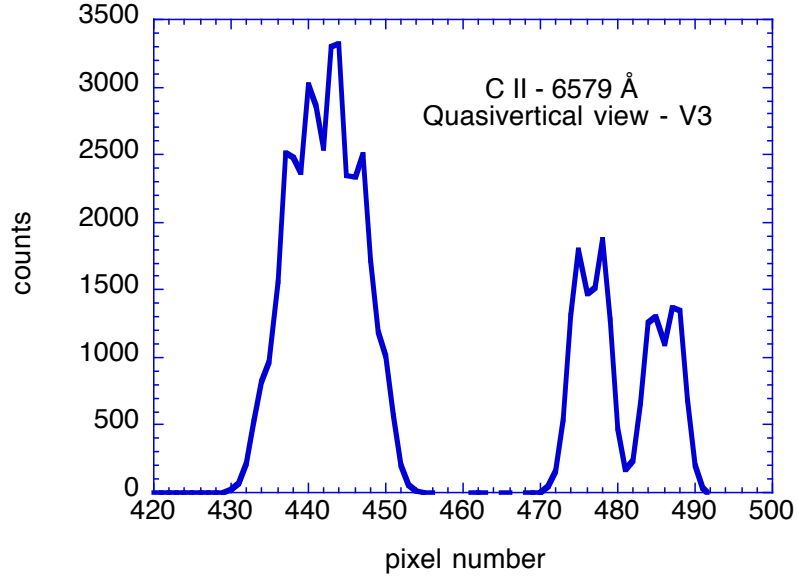

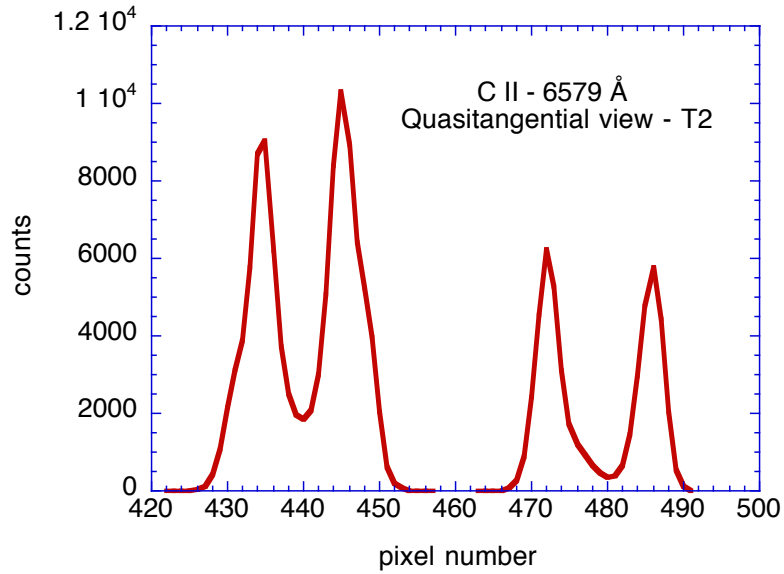

Line shift

$$\Delta\lambda = \lambda_0 \frac{v}{c} \cos\theta$$

Present vertical and tangential spectroscopic views in DIII-D

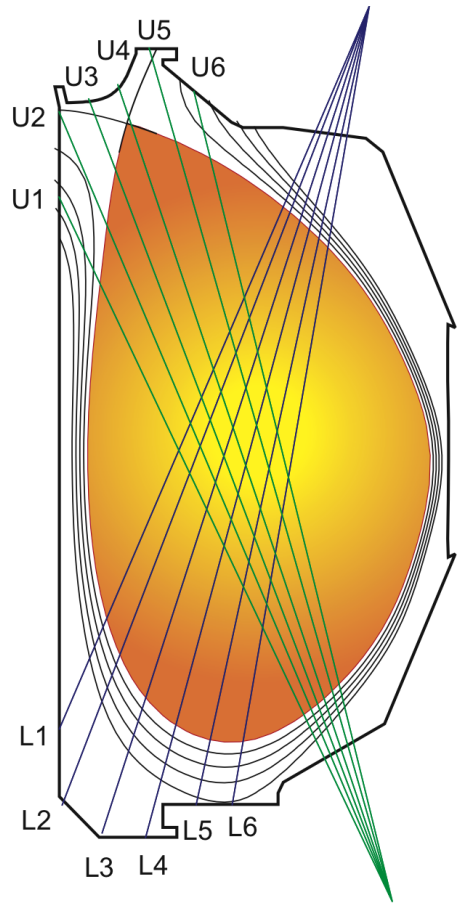

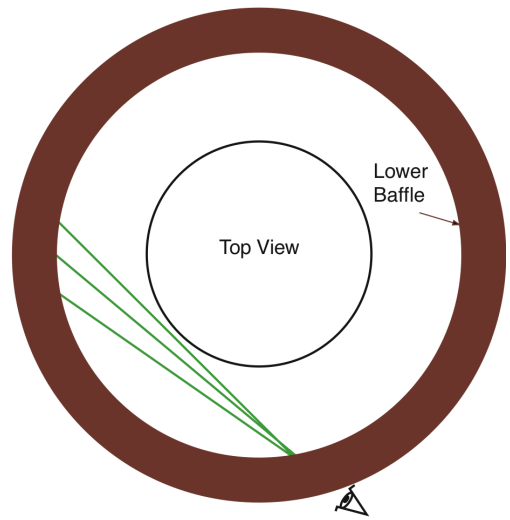

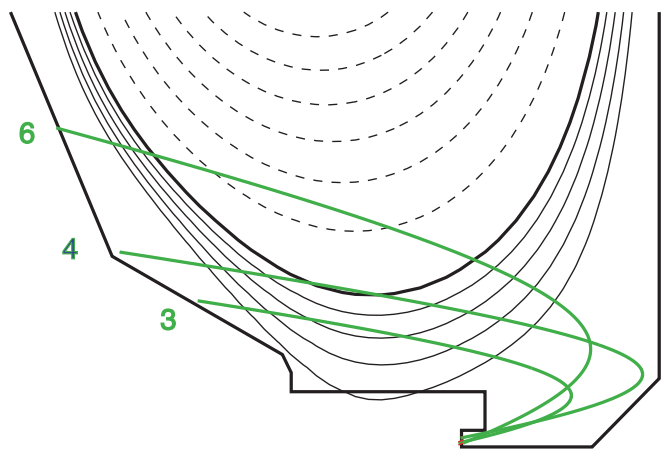

Forces on impurities

$$F_Z = -\frac{1}{n}\frac{dP}{dS} + m_Z \frac{V_{bi} - V_Z}{\tau_{sl}} + \left[0.71\, Z^2 \frac{\partial T_e}{\partial S} + \beta_Z \frac{\partial T_{bi}}{\partial S}\right] + ZeE$$

frictional force

thermal forces

Background Ions

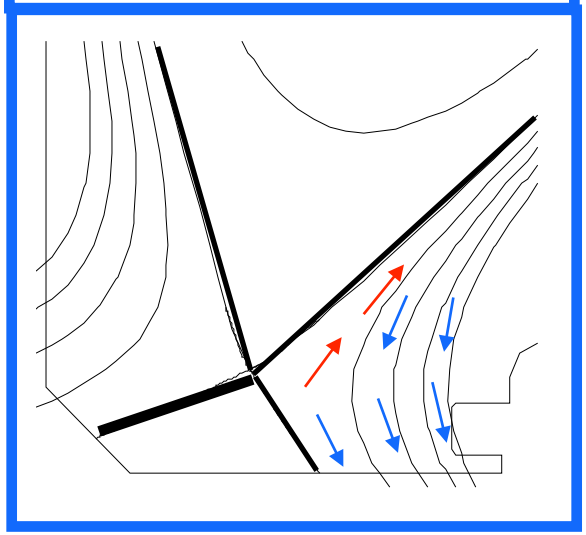

Parallel flows of B II, C II, C III, and C IV have been analyzed

C II: ^2P- ^2S profiles in normal and tangential views

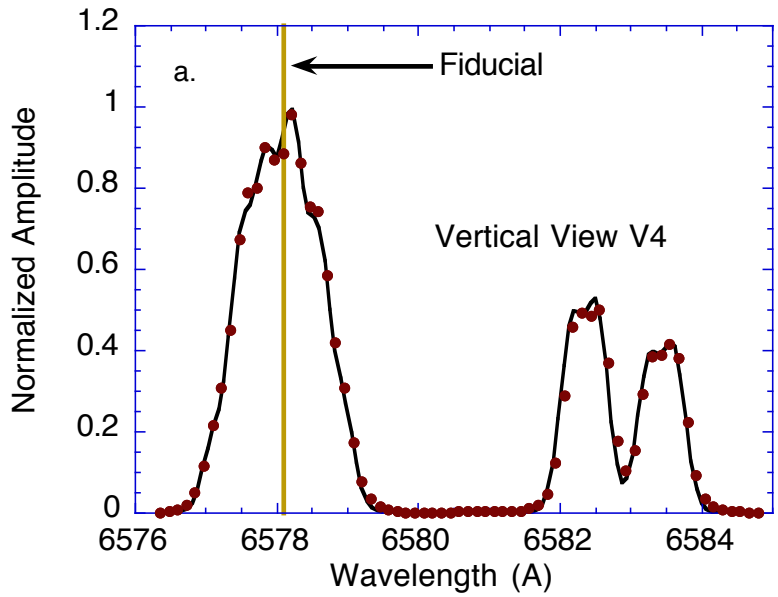

- Line profiles in tangential views often reveal significant reversed flow away from the divertor target.

- The flow speeds can change as the discharge conditions evolve.

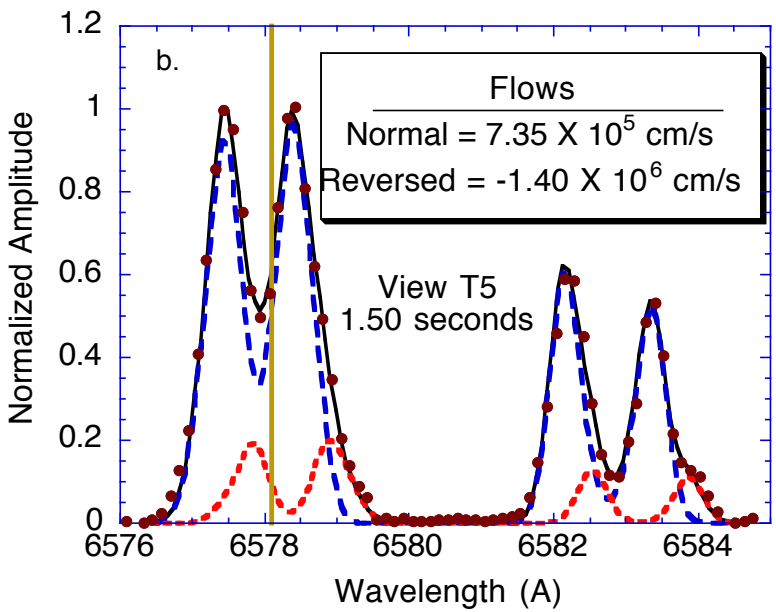

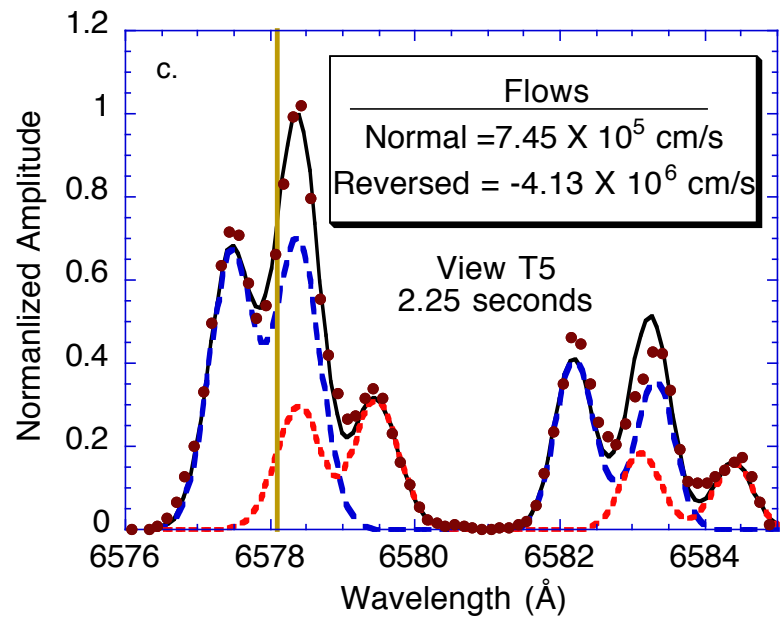

The reverse component becomes more obvious near the separatrix

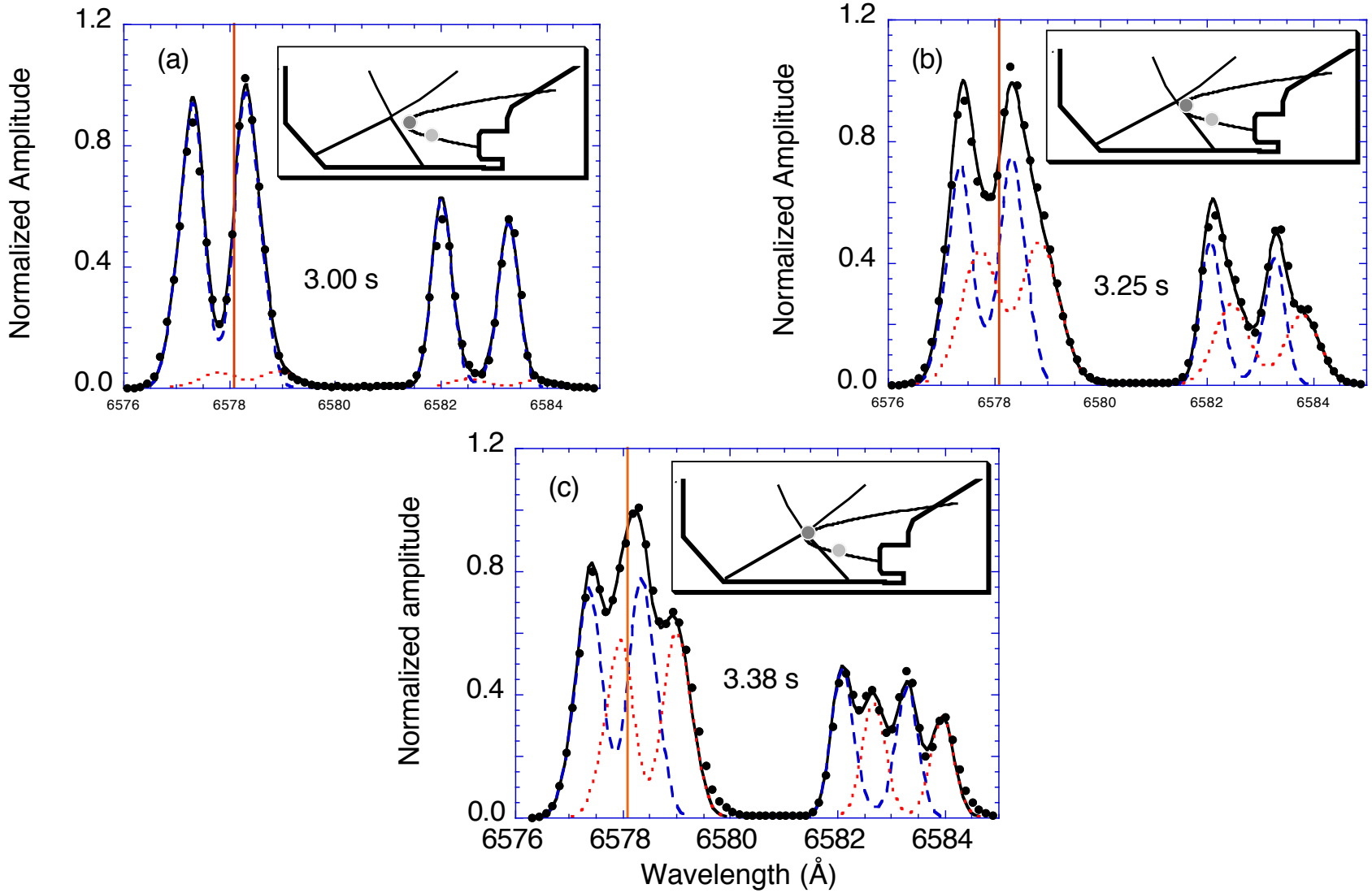

Ion temperatures and flow velocities are measured throughout the discharge

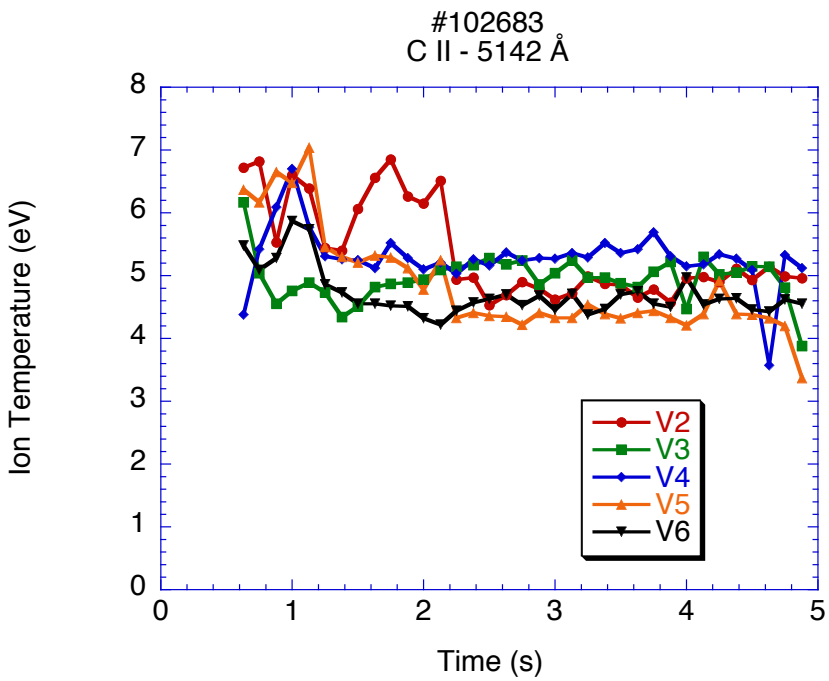

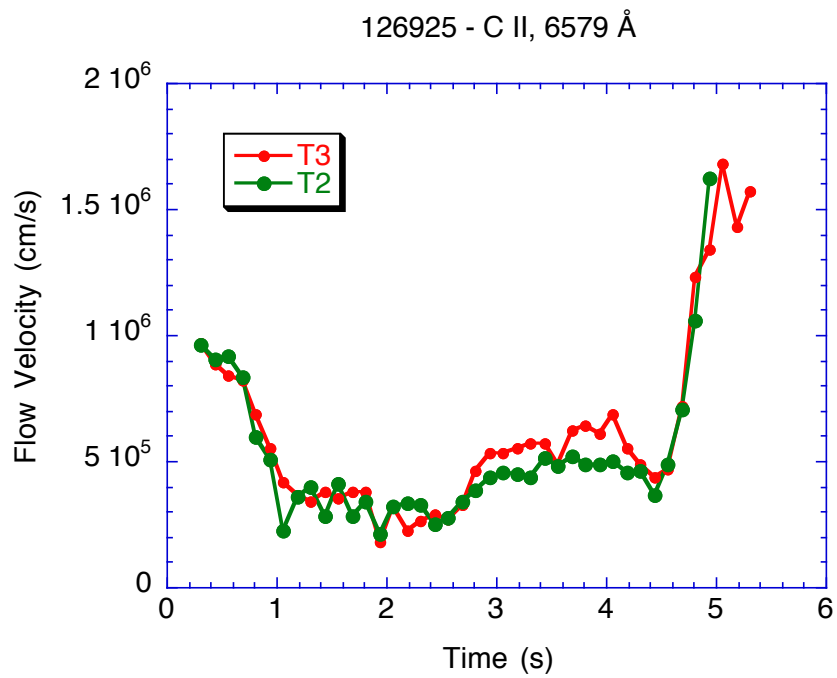

Static Electric Fields

Deuterium

(energies in wavenumbers)

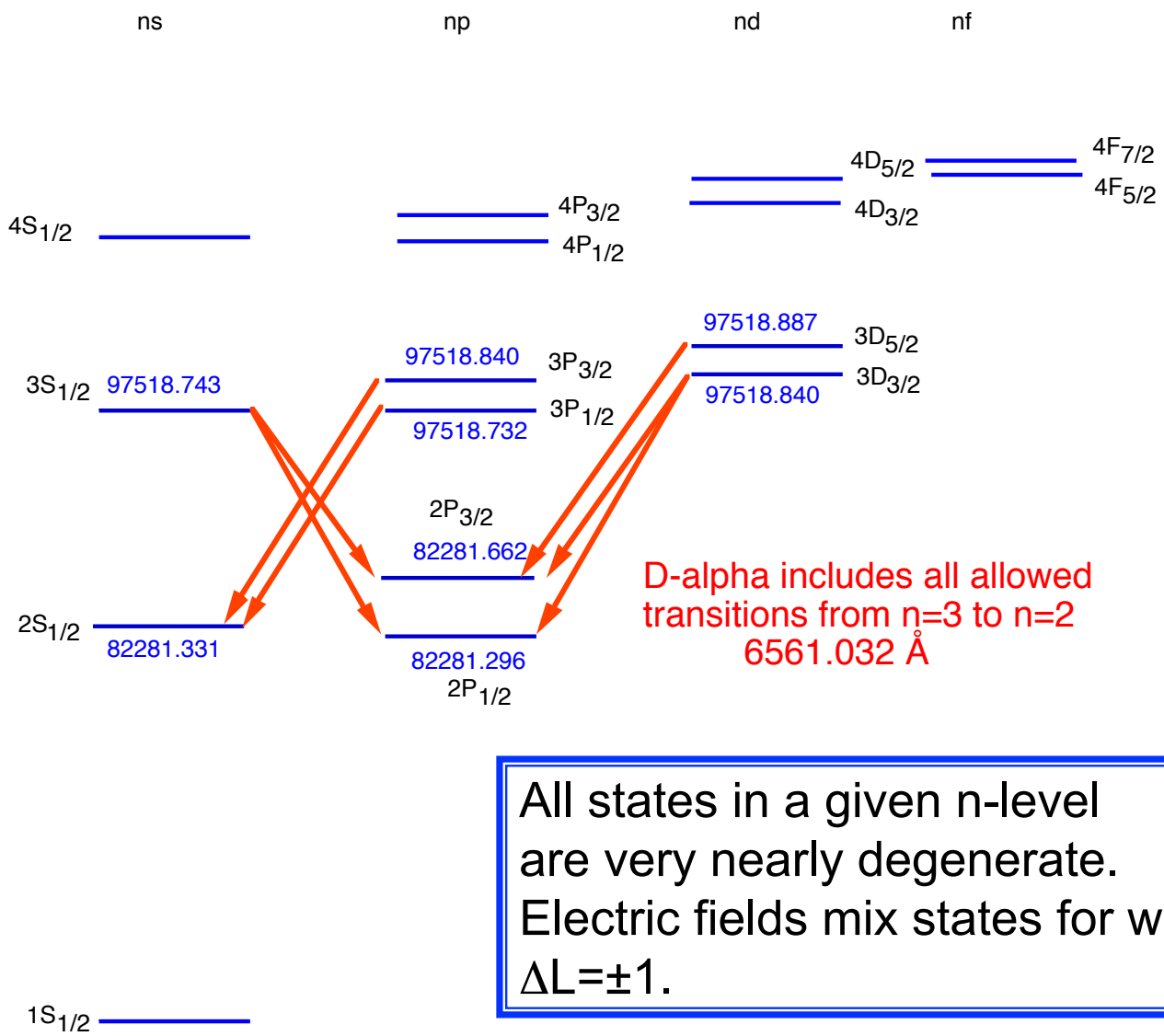

All states in a given n-level are very nearly degenerate. Electric fields mix states for which $\Delta L = \pm 1$.

If spin is neglected and the magnetic field is zero, the Schroedinger equation is separable in parabolic coordinates with or without a uniform electric field

In parabolic coordinates the substates are described by quantum numbers n_1, n_2, m rather than L,S,J, and m.

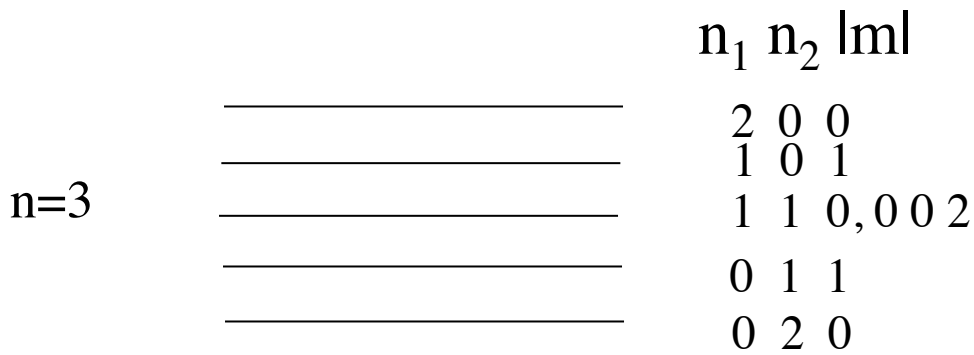

$$\Delta W = \frac{E}{15620}\frac{n}{Z}(n_1 - n_2) \quad \text{cm}^{-1}$$

These states can, of course, be written as linear combinations of states specified by L and m_l.

$$|200\rangle = -\frac{1}{\sqrt{3}}S_0^0 - \frac{1}{\sqrt{2}}P_1^0 + \frac{1}{\sqrt{6}}D_2^0$$

A comparison of Zeeman and Stark Patterns for H-alpha

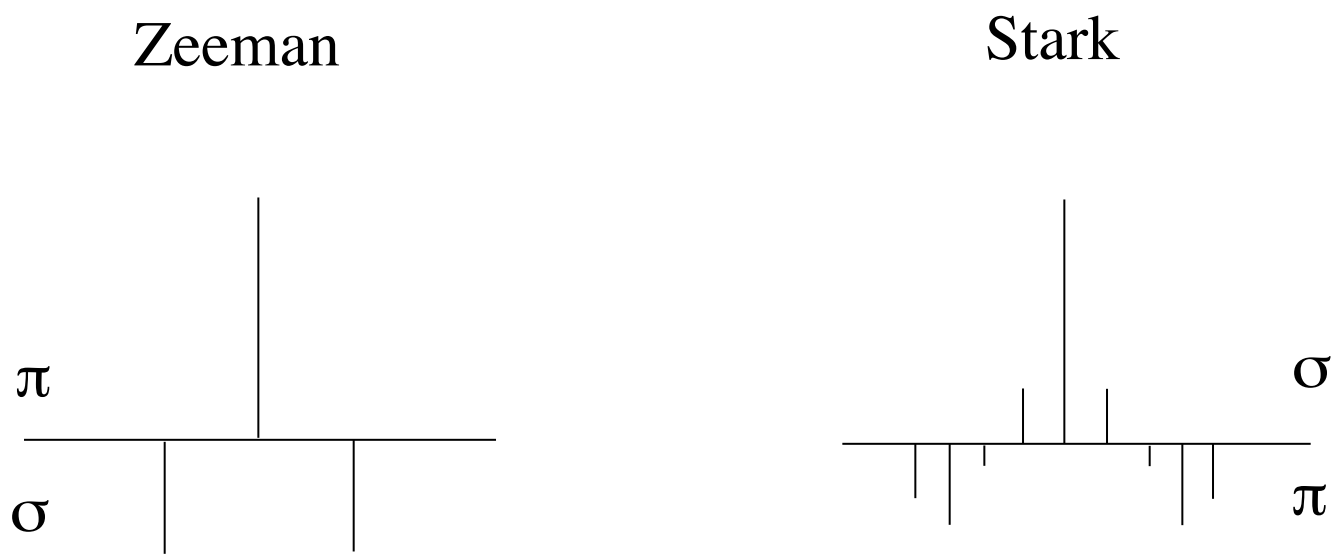

Even if the primary excitation mechanism preferentially populates certain states, you expect to see these patterns in a plasma because charged particle collisions maintain statistical populations.

Modeled D-alpha for Tore Supra Endoscope View (Gaussian Profiles)

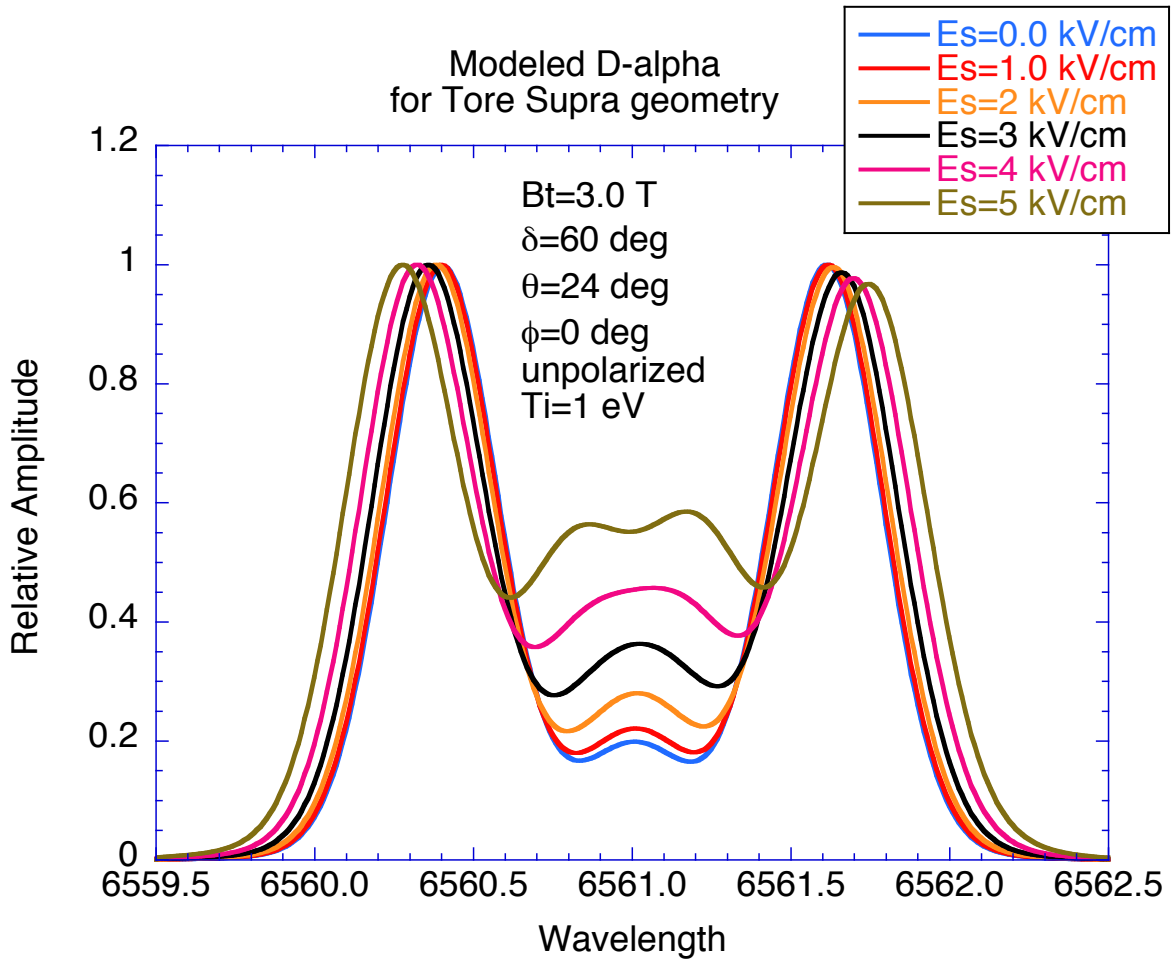

D-alpha simulations

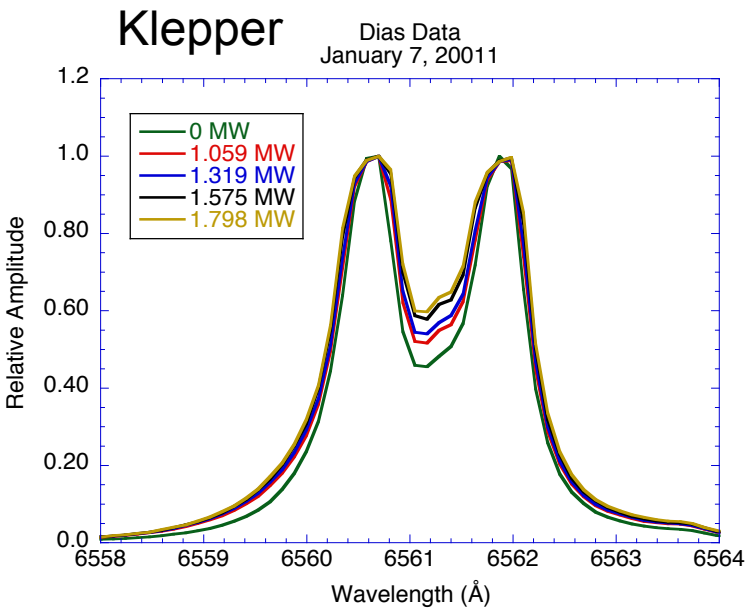

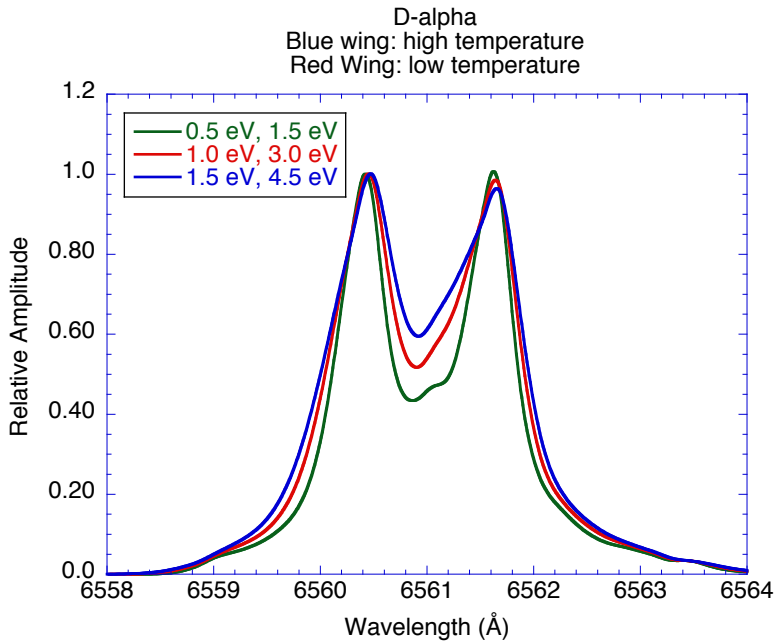

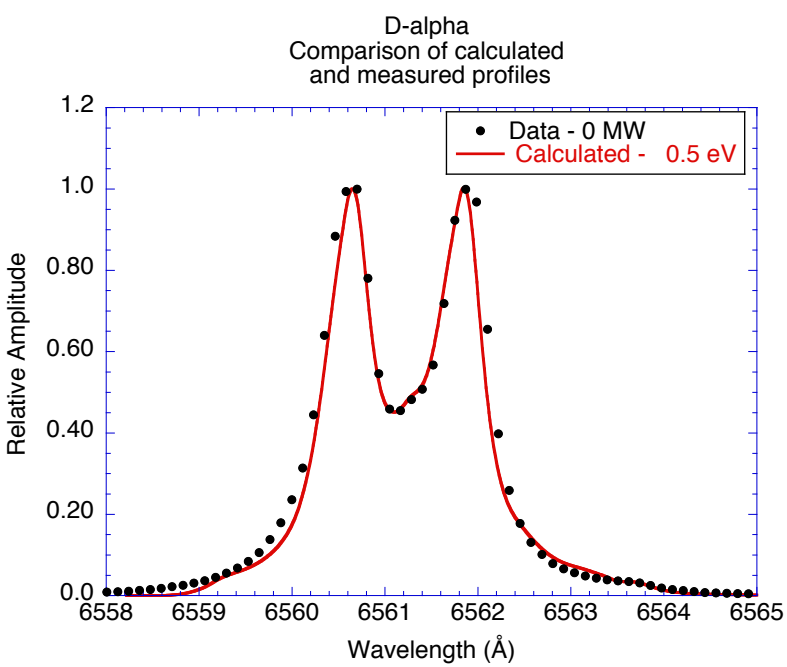

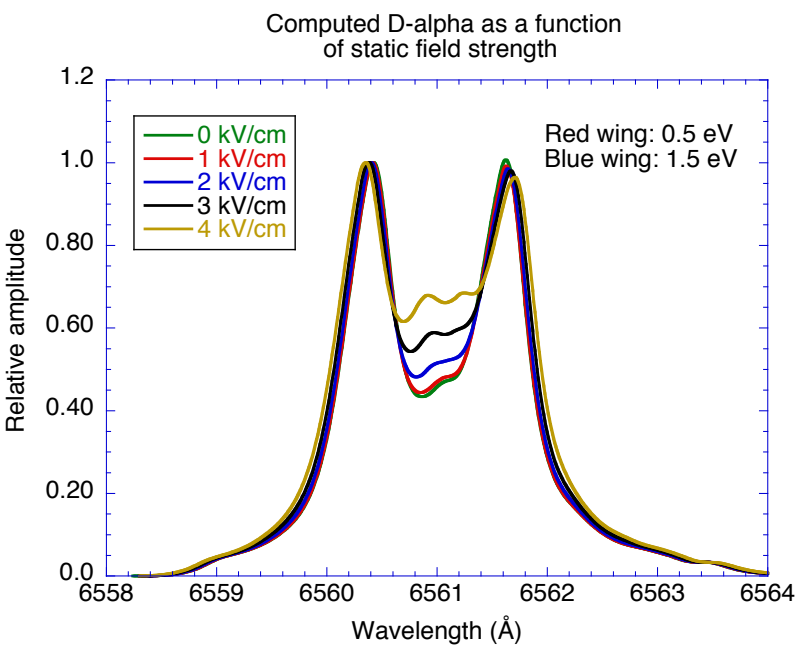

D-beta simulations

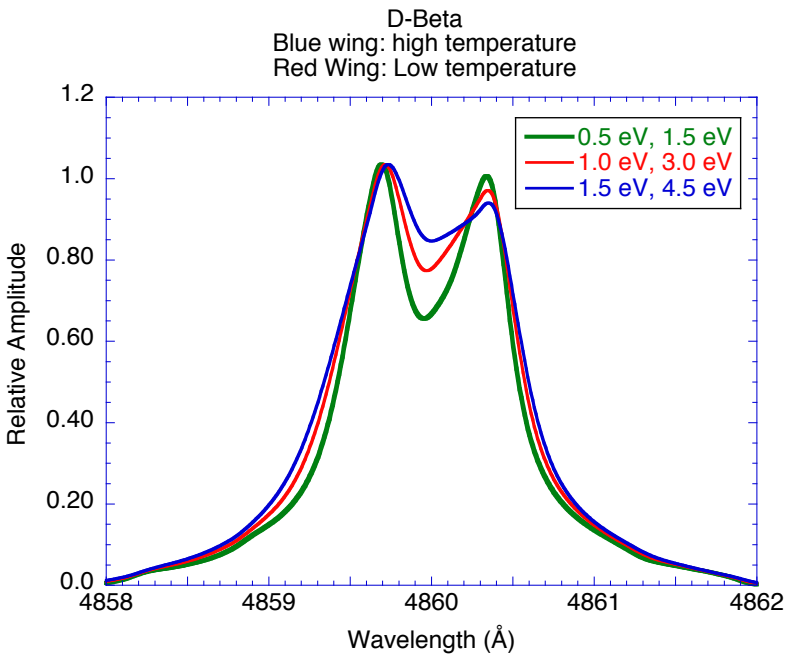

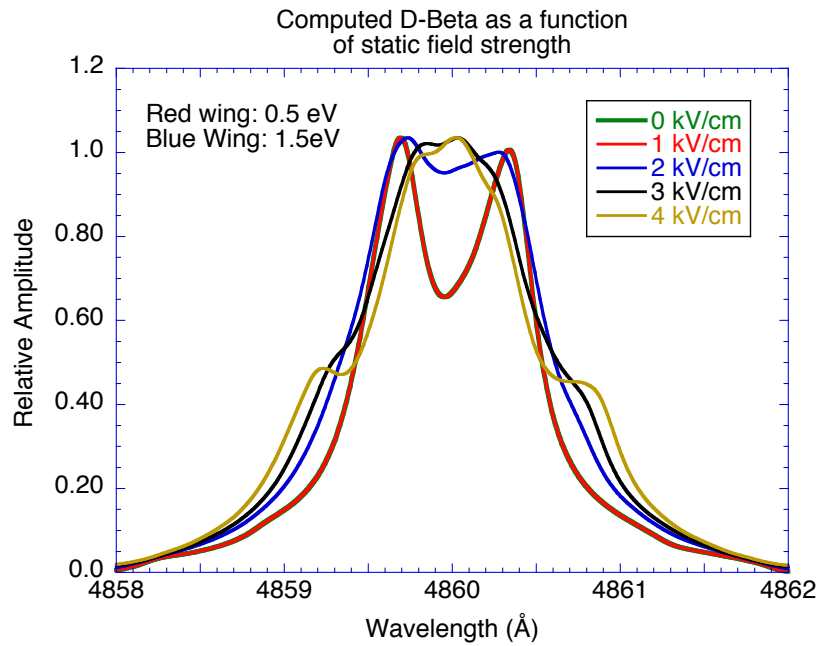

Dynamic Electric Fields

The Blochinzew Solution

For the case of zero static fields, neglected fine-structure, and a dynamic field $E = E_0 \cos\omega_{rf} t$. Blochinzew obtained solutions

$$I(\omega - \omega_0) \propto \sum_{p=-\infty}^{p=\infty} \delta(\omega - \omega_0 - p\omega_{rf}) \left[f_0 \delta_{p0} + 2 \sum_{k=1}^{k\,\max} f_k J_p^2(X_k \varepsilon) \right]$$

where $X_k\varepsilon$ is the difference of the upper and lower Stark splittings divided by the energy of the rf photon. J_p is a Bessel function of order p, and the f's are the intensities of the Stark components in a static field of strength E_0.

Examples

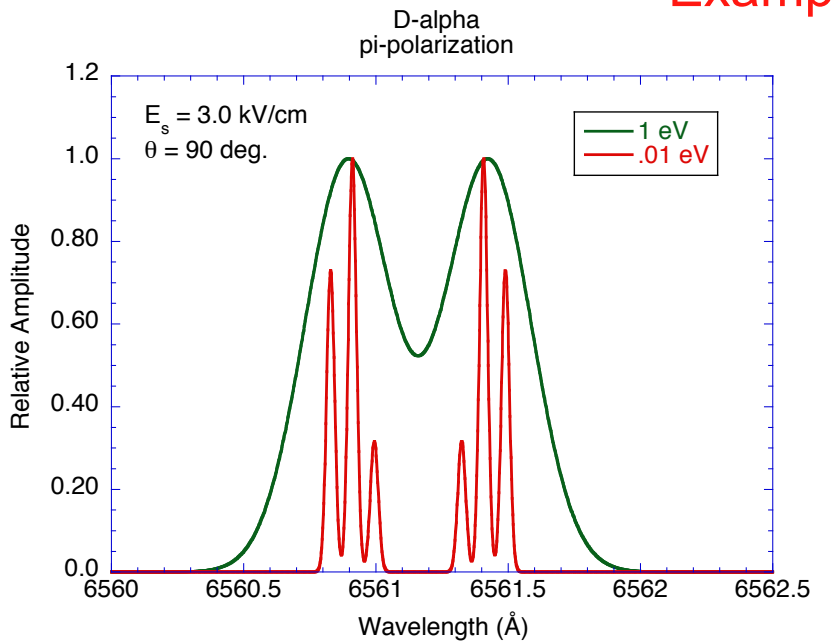
D-alpha
pi-polarization
E_s = 3.0 kV/cm
θ = 90 deg.
1 eV
.01 eV
Relative Amplitude
Wavelength (Å)

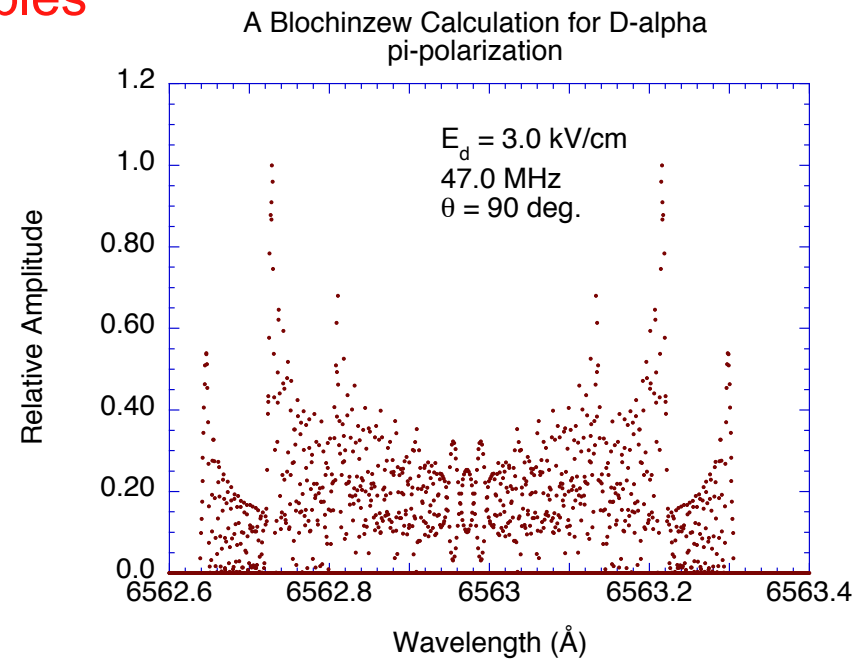
A Blochinzew Calculation for D-alpha
pi-polarization
E_d = 3.0 kV/cm
47.0 MHz
θ = 90 deg.
Relative Amplitude
Wavelength (Å)

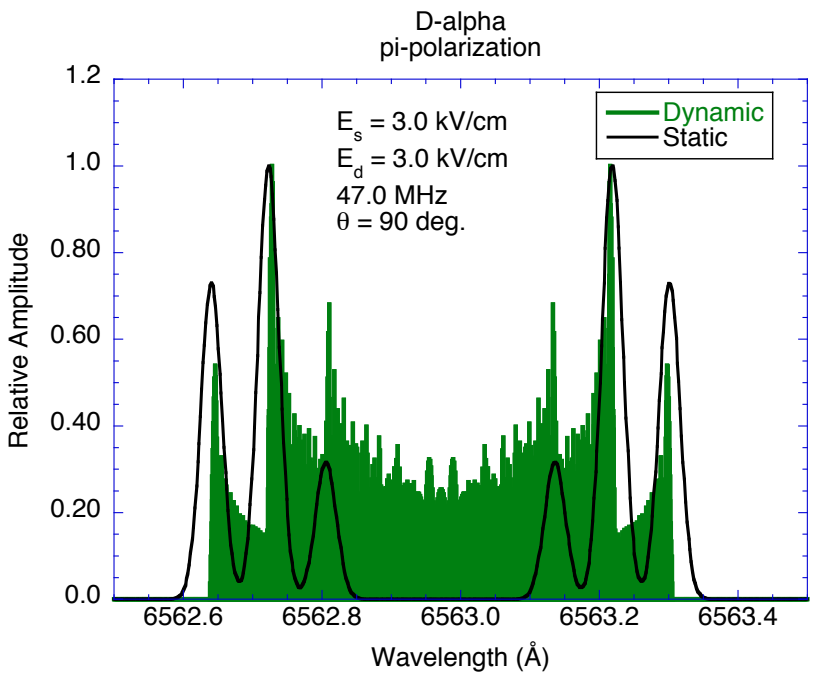
D-alpha
pi-polarization
E_s = 3.0 kV/cm
E_d = 3.0 kV/cm
47.0 MHz
θ = 90 deg.
Dynamic
Static
Relative Amplitude
Wavelength (Å)

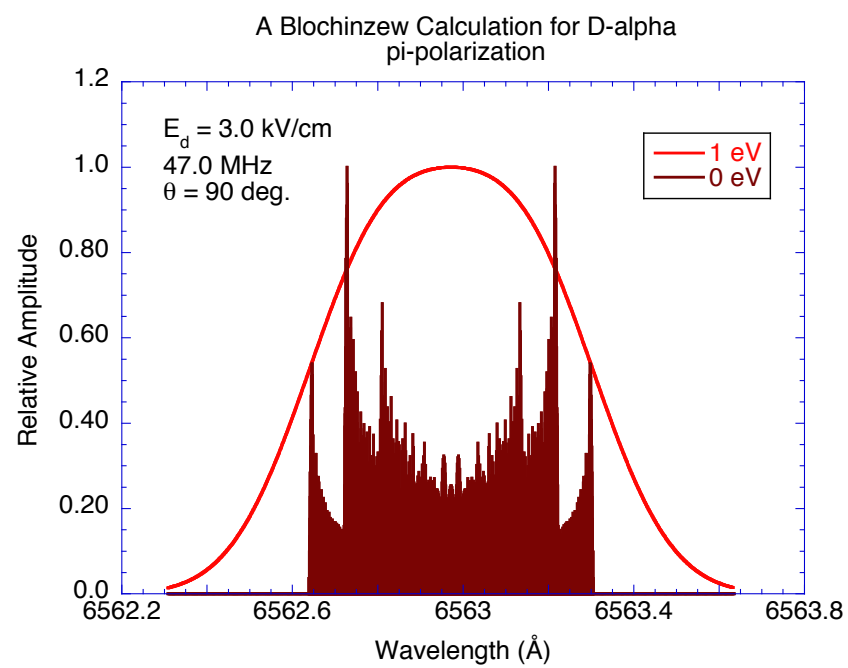
A Blochinzew Calculation for D-alpha
pi-polarization
E_d = 3.0 kV/cm
47.0 MHz
θ = 90 deg.
1 eV
0 eV
Relative Amplitude
Wavelength (Å)

The time-dependent Schroedinger Equation

$$i\hbar \frac{\partial \Psi}{\partial t} = \underbrace{(H_0 + H_{fs} + H_B + H_{Es}}_{\text{Static field terms}} + H_{Ed})\Psi$$

$$H_{Ed} = E_d \cos \omega t$$

The time independent eigenfunctions of H_0 and H_{fs} form a set of basis states U_k {<S L J m_j|} so the complete solution of the time-dependent equation can be expanded as

$$\Psi = \sum_{j=1}^{N} T_j(t) U_j$$

Inserting this expression into the time dependent Schroedinger equation, multiplying by U_k from the left, and integrating over the spatial coordinates gives

$$i\hbar \frac{\partial T_k}{\partial t} = E_k T_k + \sum_{j=1}^{N} (\beta_{kj} + \gamma_{kj} e^{i\omega t} + \gamma_{kj} e^{-i\omega t})$$

$$\beta_{kj} = \left\langle U_k \middle| \zeta \vec{L} \bullet \vec{S} + \mu_b \vec{B} \bullet (\vec{L} + 2\vec{S}) + e\vec{E}_s \bullet \vec{r} \middle| U_j \right\rangle$$

$$\gamma_{kj} = \left\langle U_k \middle| 0.5\, \vec{E}_D \bullet \vec{r} \middle| U_j \right\rangle$$

Floquet's Theorem allows the coefficients T_k to be expanded in powers of $e^{\iota\omega t}$

$$T_k = e^{-i\lambda t} \sum_{s=-\infty}^{\infty} C_{ks} e^{-is\omega t}$$

Substitution and separation of terms with equal powers of ω gives

$$\left(E_k - s\hbar\omega - \lambda\right)C_{ks} + \sum_{j=1}^{N}\left(\beta_{kj}C_{js} + \gamma_{kj}C_{j\,s+1} + \gamma_{kj}C_{j\,s+1}\right) = 0$$

$$k = 1, N \qquad s = -\infty \ldots\ldots\ldots + \infty$$

$$C_{ks} = 0 \; for \; |s| > M$$

There are N linearly independent solutions with 2M+1 members in each set.

$$\Psi_k = e^{-i\lambda_k t} \sum_{j=1}^{N} C_{js}^{k} e^{-is\omega t} U_j$$

The Floquet matrix

	s=-2	s=-1	s=0	s=+1	s=+2
s=-2	$\mathbf{A}-2\omega\mathbf{1}$	$\mathbf{B}/2$			
s=-1	$\mathbf{B}/2$	$\mathbf{A}-\omega\mathbf{1}$	$\mathbf{B}/2$		
s=0		$\mathbf{B}/2$	$\mathbf{A}$	$\mathbf{B}/2$	
s=+1			$\mathbf{B}/2$	$\mathbf{A}+\omega\mathbf{1}$	$\mathbf{B}/2$
s=+2				$\mathbf{B}/2$	$\mathbf{A}+2\omega\mathbf{1}$

The C's are found by solving the eigenvalue problem for the Floquet matrix. **A**, **B**, and **1** are m x m matrices where m = the degeneracy of the hydrogenic level. For the n = 3 level, m = 18. Thus, there 90 eigenvalues and eigenfunctions for this 90 x 90 matrix. Only 18 are to be used to calculated the spectrum. Which 18 to use is not obvious. Also,it may be necessary to choose M, the maximum s, to be much larger than 2.

Line intensities for D-alpha, s = -3 to s = +3

Eigenvalues of Floquet matrices

$$L(\omega_\gamma) = \sum_{f=1}^{8}\sum_{i=1}^{18}\sum_{s,s'=-3}^{3}\delta(\omega_\gamma + \lambda_f - \lambda_i + s'\omega - s\omega)\sum_{\tilde{s},\tilde{s}'=-3}^{3}\delta((s-s')-(\tilde{s}-\tilde{s}'))\bullet$$

$$\left\langle \sum_{j=1}^{18} C_{js}^{i} U_j^i \left|\vec{\varepsilon}\bullet\vec{d}\right| \sum_{k=1}^{8} C_{ks'}^{f} U_k^f \right\rangle \left\langle \sum_{j=1}^{18} C_{j\tilde{s}}^{i} U_j^i \left|\vec{\varepsilon}\bullet\vec{d}\right| \sum_{k=1}^{8} C_{k\tilde{s}'}^{f} U_k^f \right\rangle$$

The number of transitions is 8 x 18 x 7 = 1008

The Blochinzew and Floquet calculations agree for the Lyman series

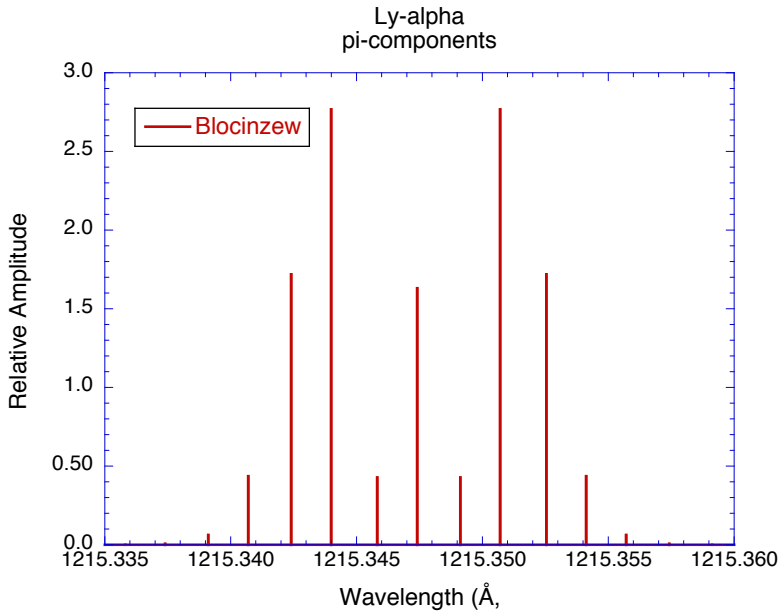

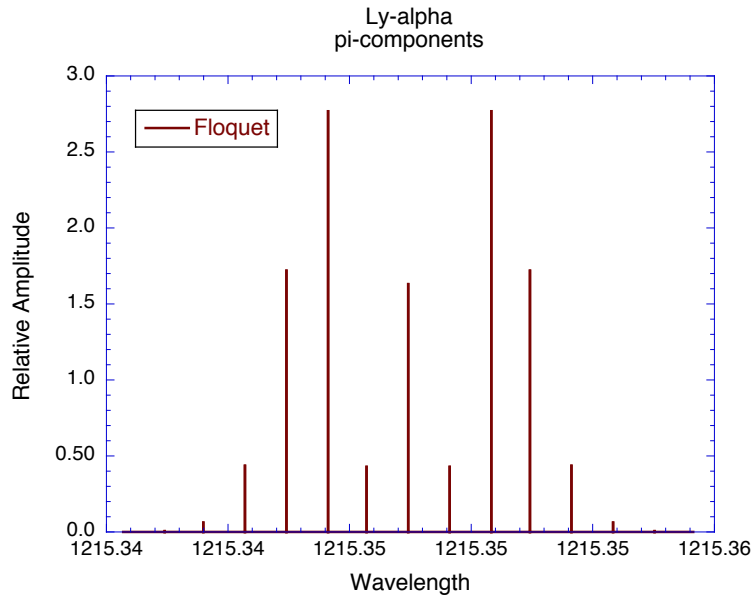

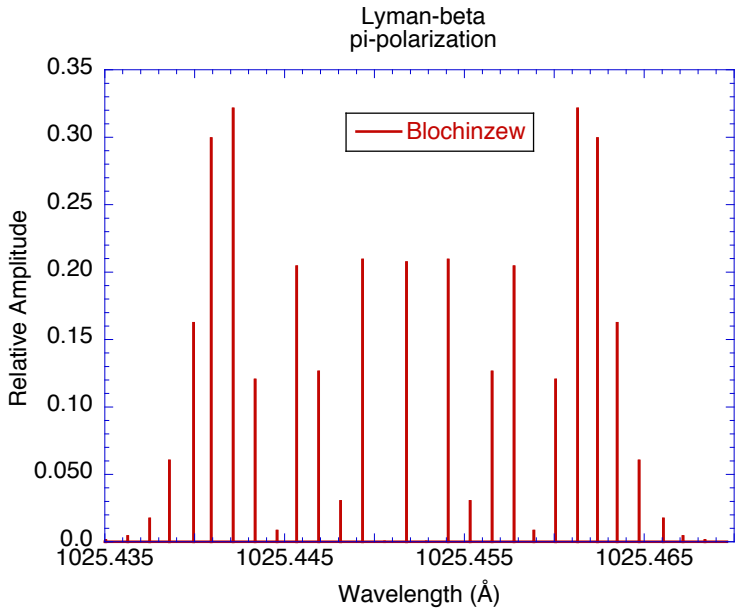

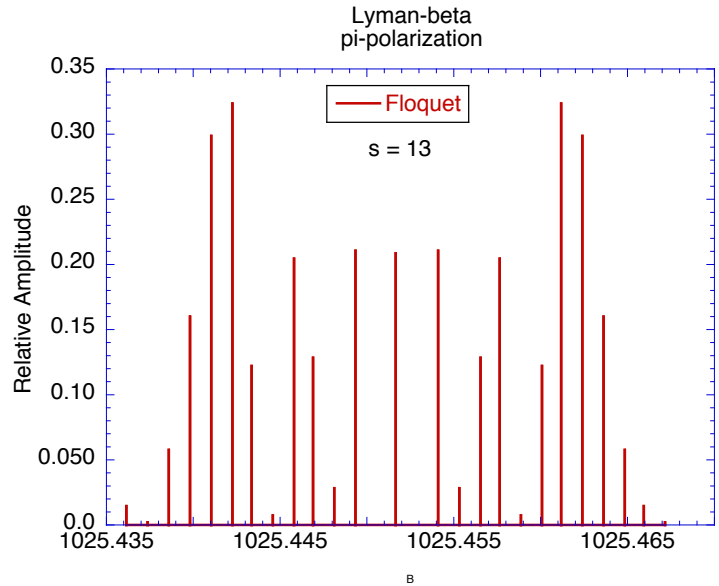

D-alpha spectrum for the Blochinzew and Floquet formalisms

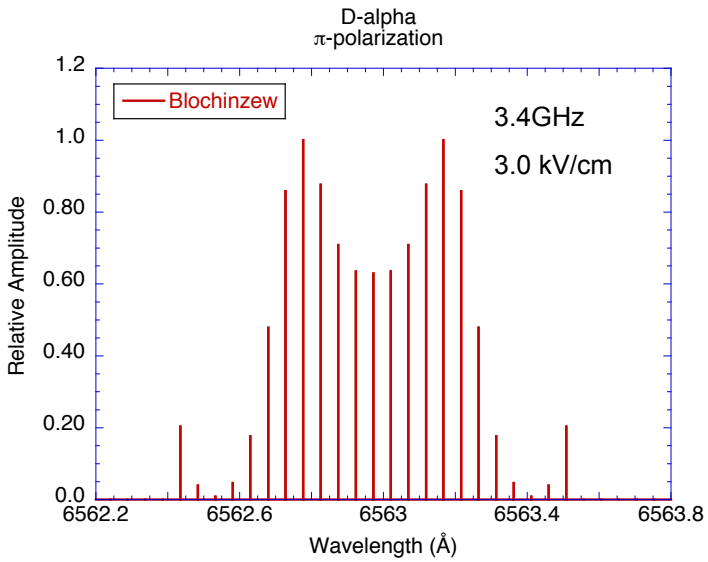

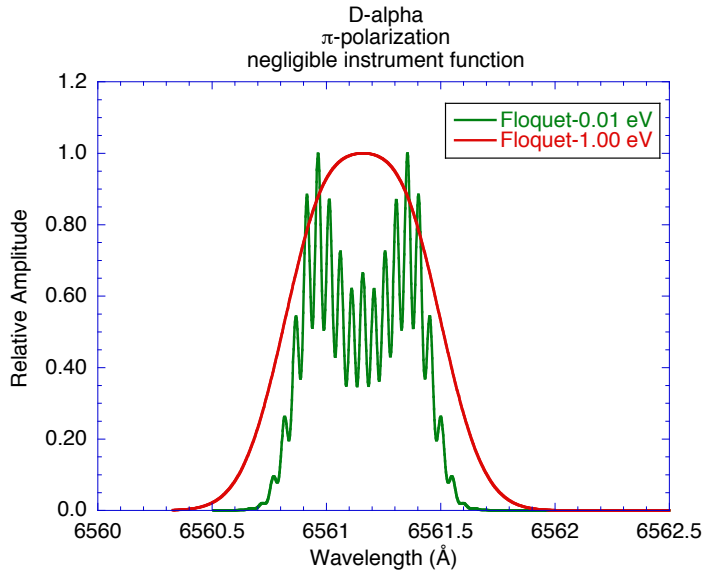

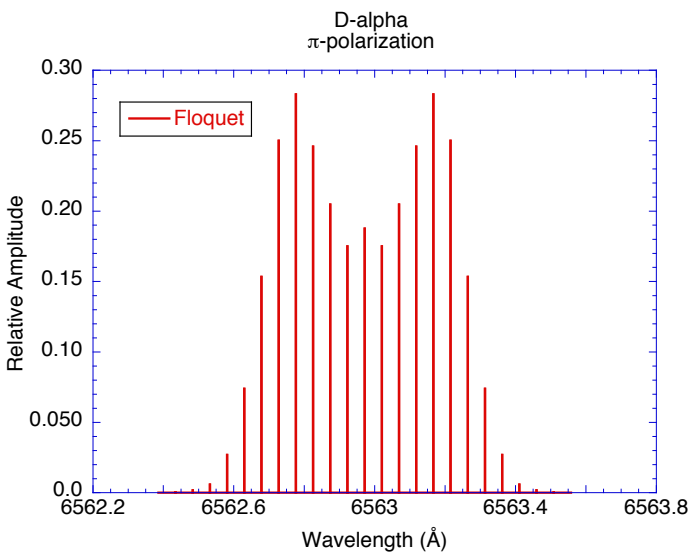

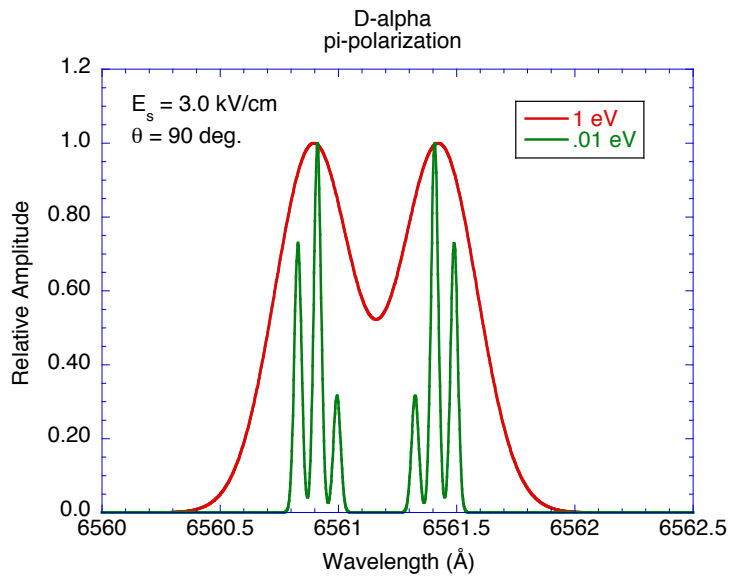

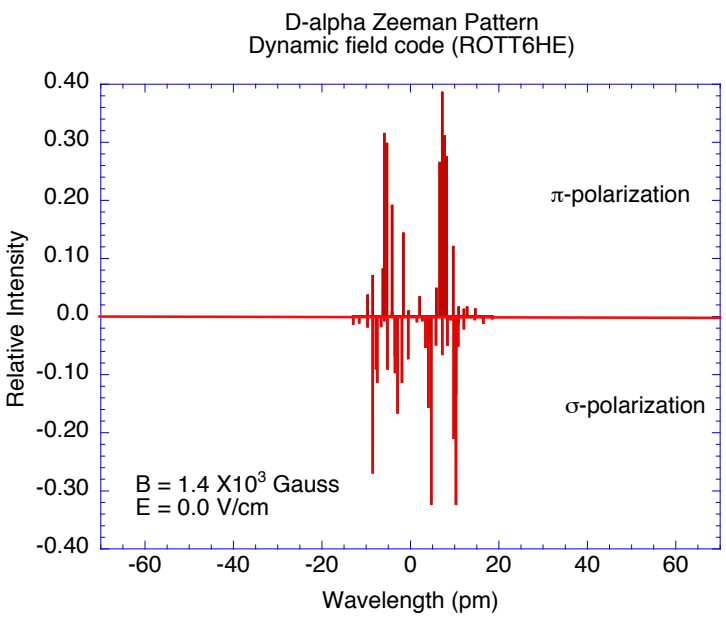
D-alpha Zeeman Pattern
Dynamic field code (ROTT6HE)
Relative Intensity
Wavelength (pm)
π-polarization
σ-polarization
B = 1.4 X10^3 Gauss
E = 0.0 V/cm

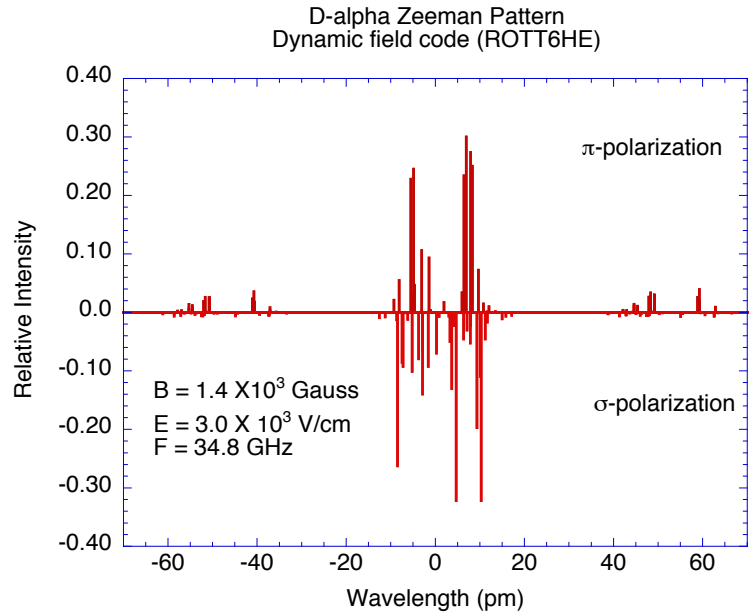
D-alpha Zeeman Pattern
Dynamic field code (ROTT6HE)
Relative Intensity
Wavelength (pm)
π-polarization
σ-polarization
B = 1.4 X10^3 Gauss
E = 3.0 X 10^3 V/cm
F = 34.8 GHz

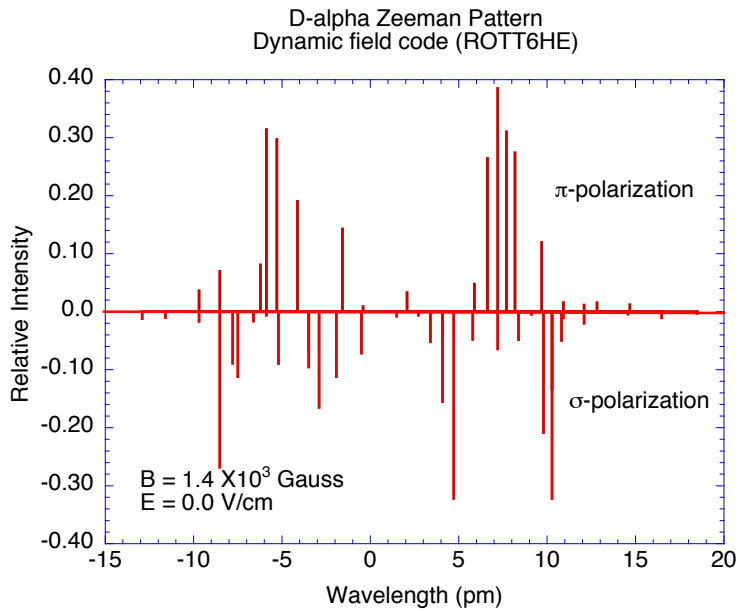
D-alpha Zeeman Pattern
Dynamic field code (ROTT6HE)
Relative Intensity
Wavelength (pm)
π-polarization
σ-polarization
B = 1.4 X10^3 Gauss
E = 0.0 V/cm

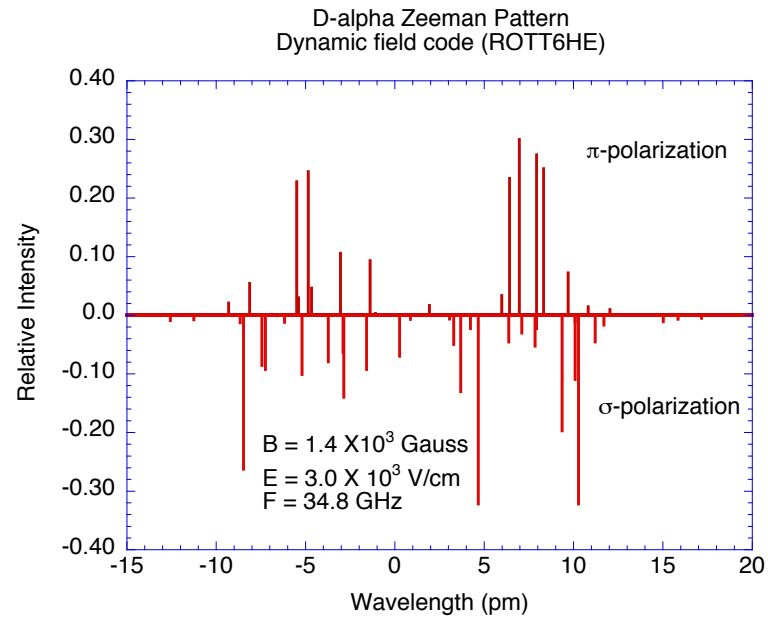
D-alpha Zeeman Pattern
Dynamic field code (ROTT6HE)
Relative Intensity
Wavelength (pm)
π-polarization
σ-polarization
B = 1.4 X10^3 Gauss
E = 3.0 X 10^3 V/cm
F = 34.8 GHz

Central Pattern of D-alpha

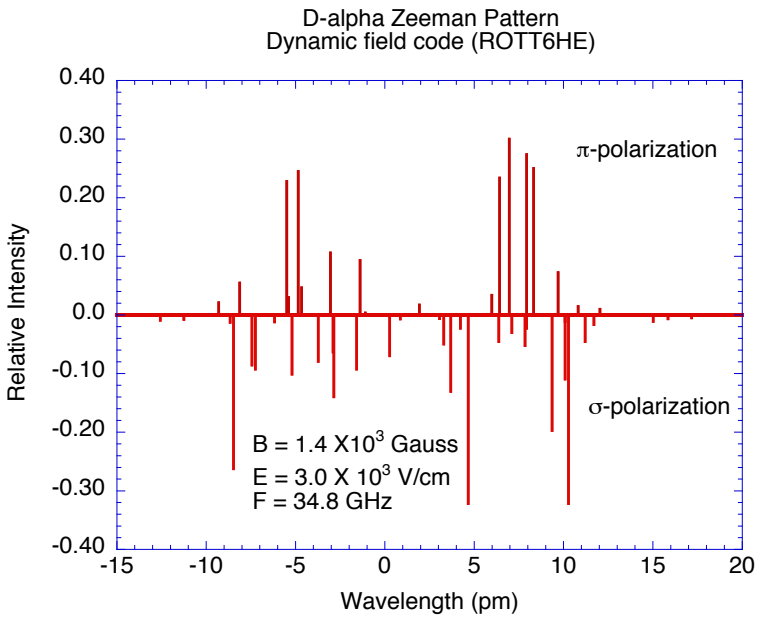

Hirsch and Himmel

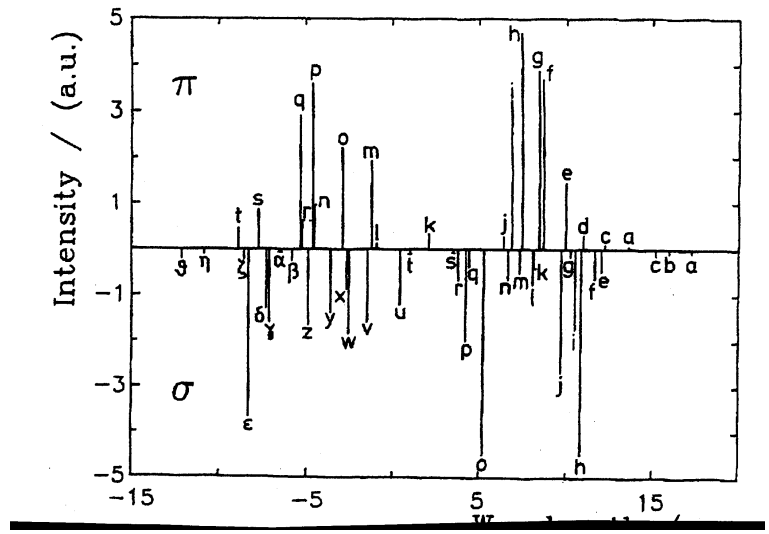

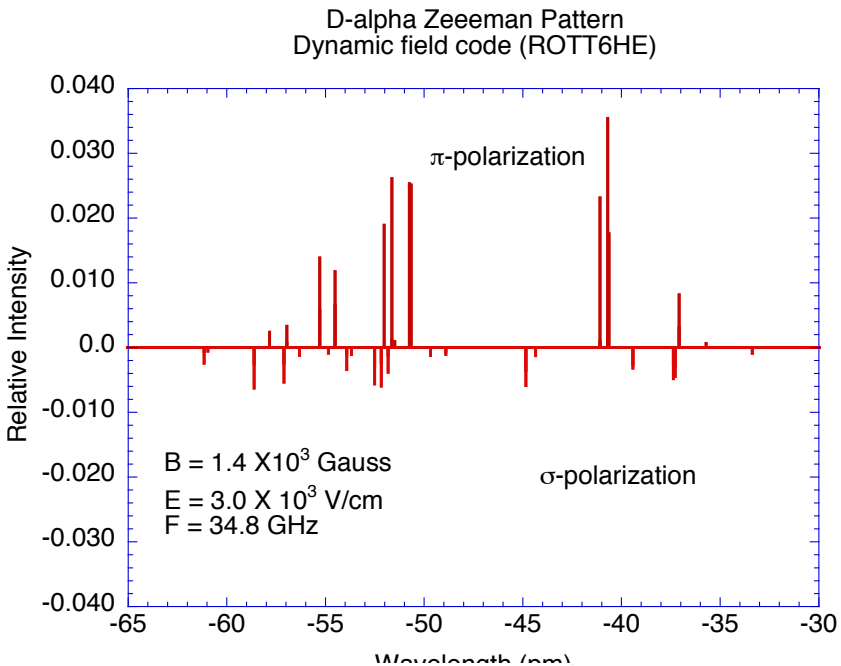

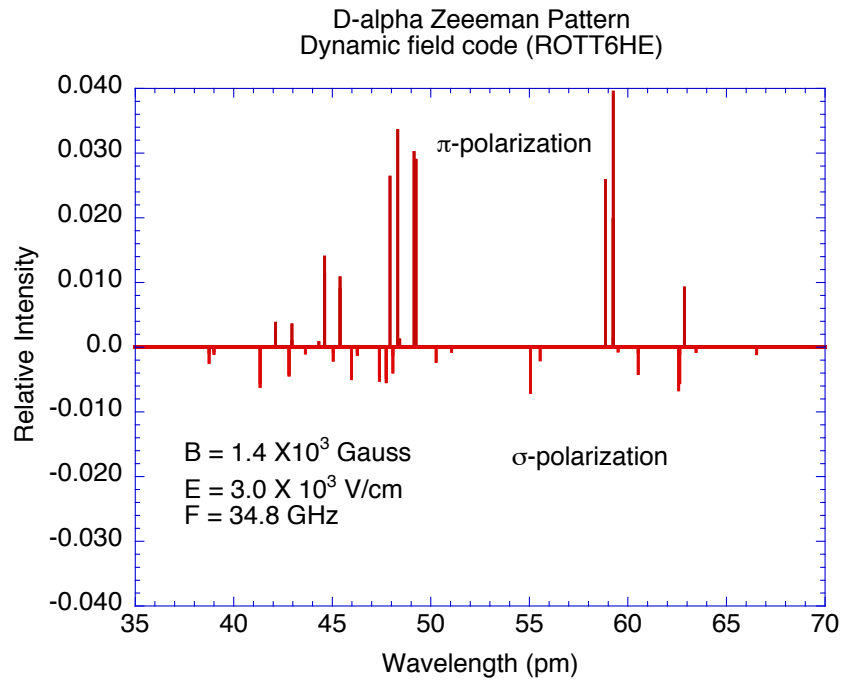

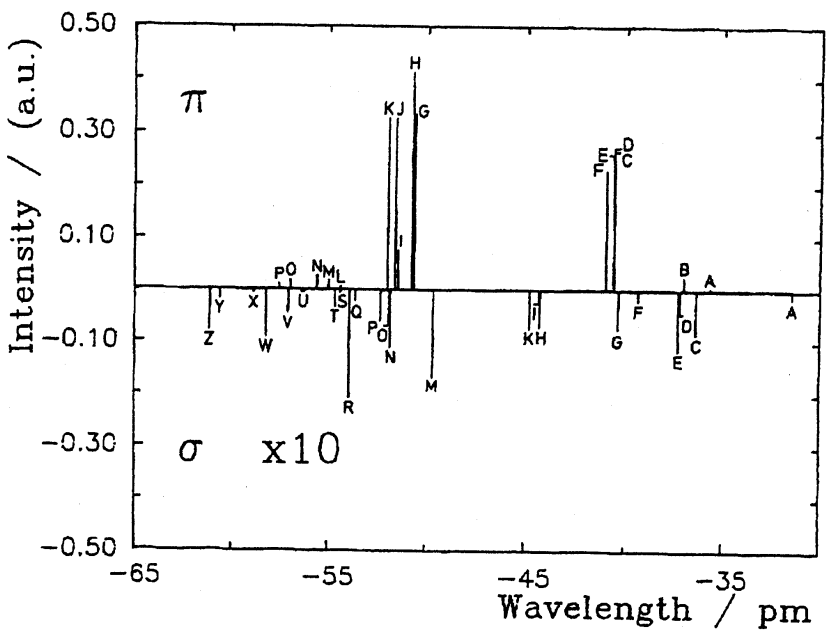

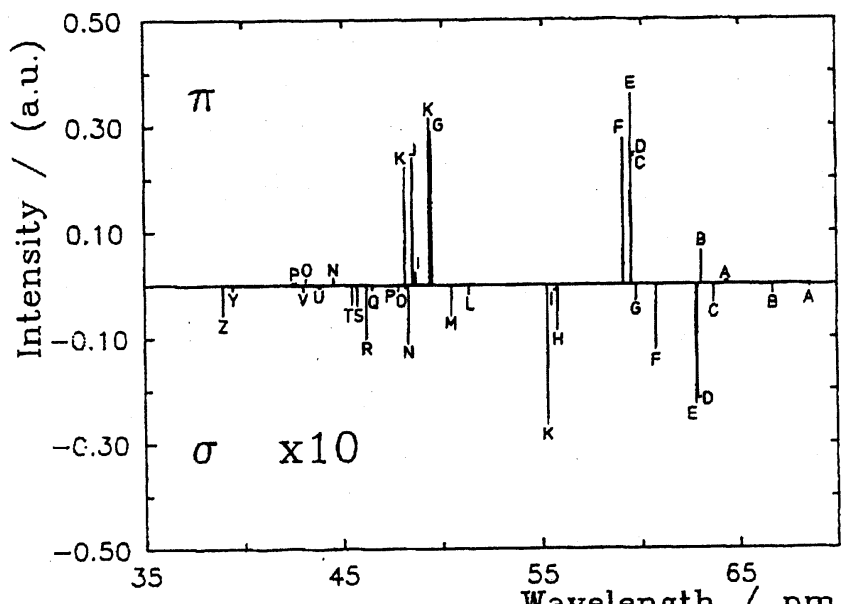

Hirsch and Himmel

Modeled deuterium lines for the Tore Supra DIAS experiment

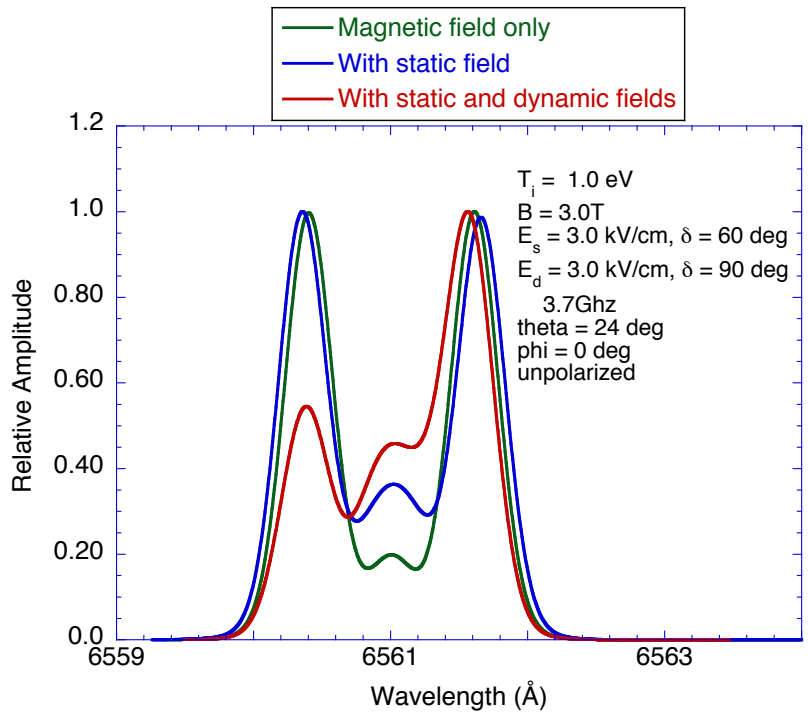

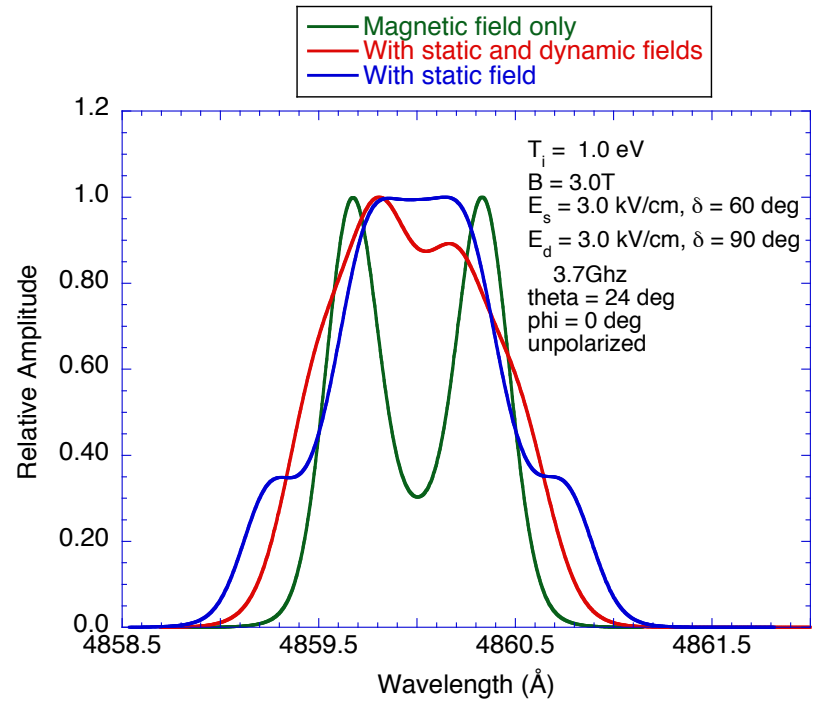

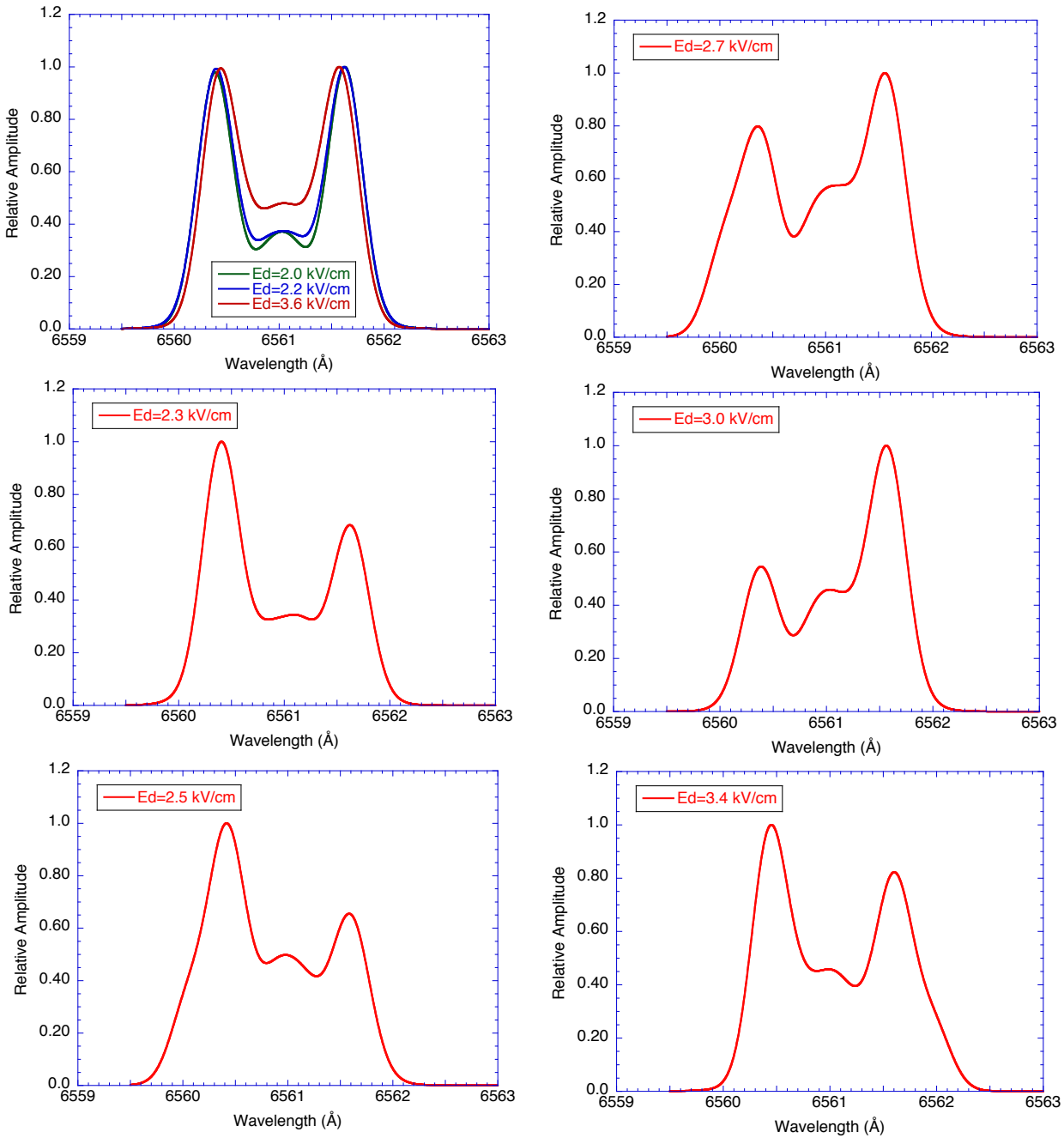

Modeled D-alpha profiles for various values of the dynamic electric field

Helium

A He I Grotrian Diagram

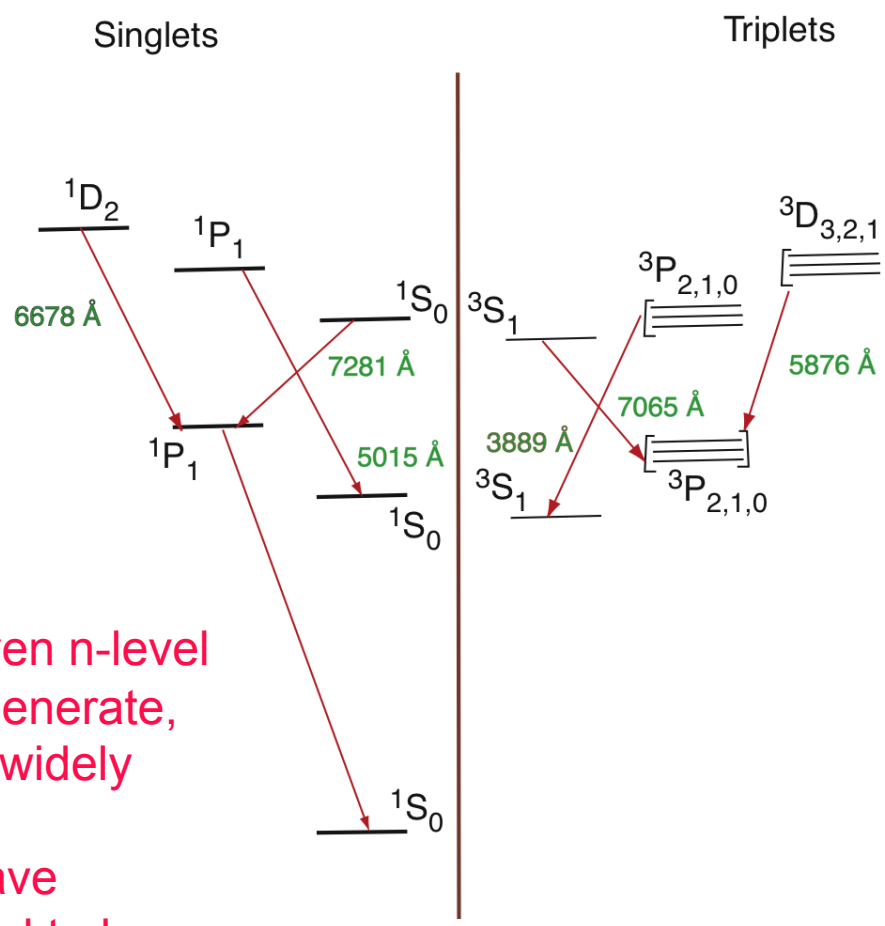

The L-states for a given n-level of helium are not degenerate, but they also are not widely separated. For a first approximation,the wave functions are assumed to be hydrogenic.

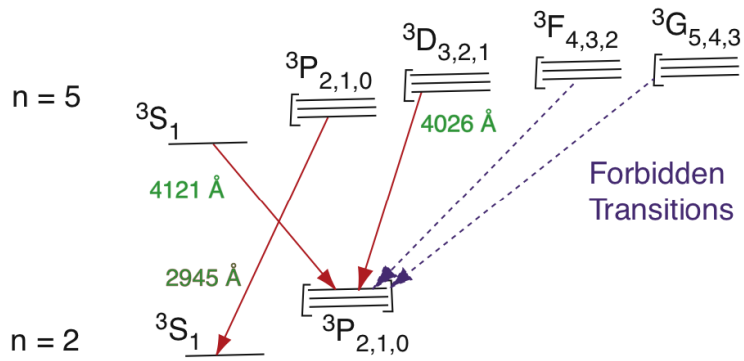

Static electric fields give rise to forbidden satellite lines in helium.

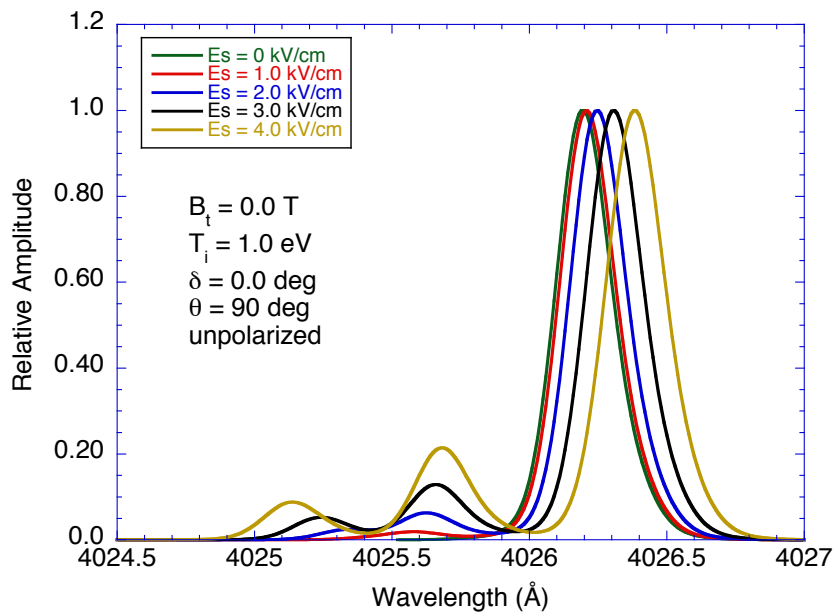

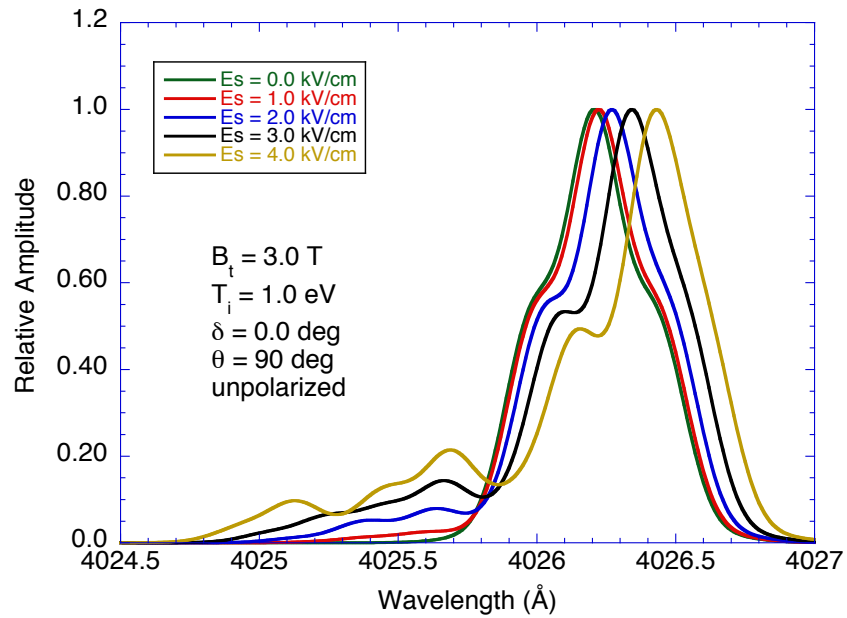

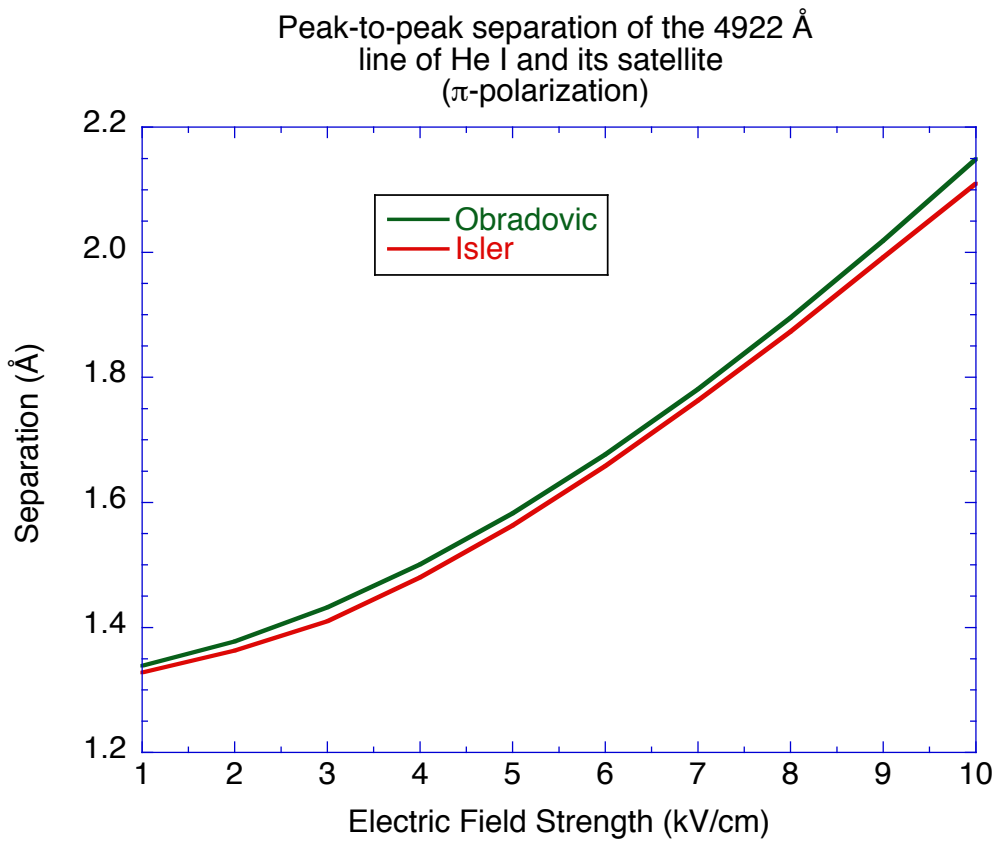
Peak-to-peak separation of the 4922 Å
line of He I and its satellite
(π-polarization)
Obradovic
Isler
Separation (Å)
2.2
2.0
1.8
1.6
1.4
1.2
1
2
3
4
5
6
7
8
9
10
Electric Field Strength (kV/cm)

Carbon Release Mechanisms

Non-isotropic distributions

Maxwellian hemisphere

Normal View

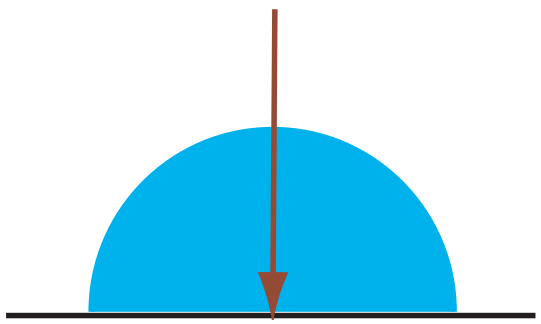

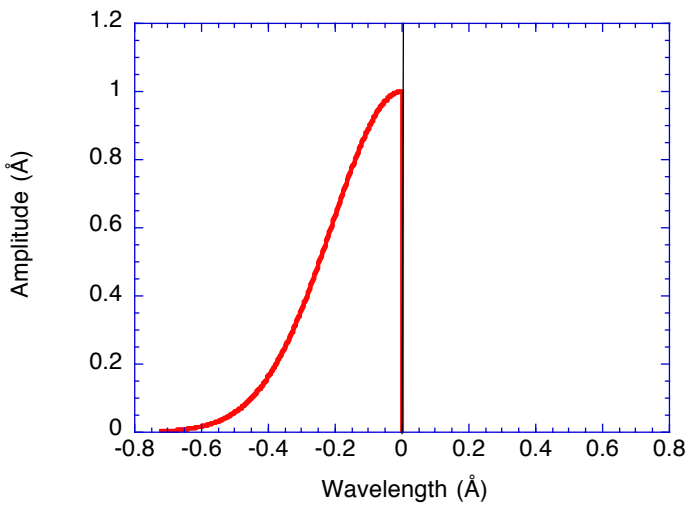

Angled View

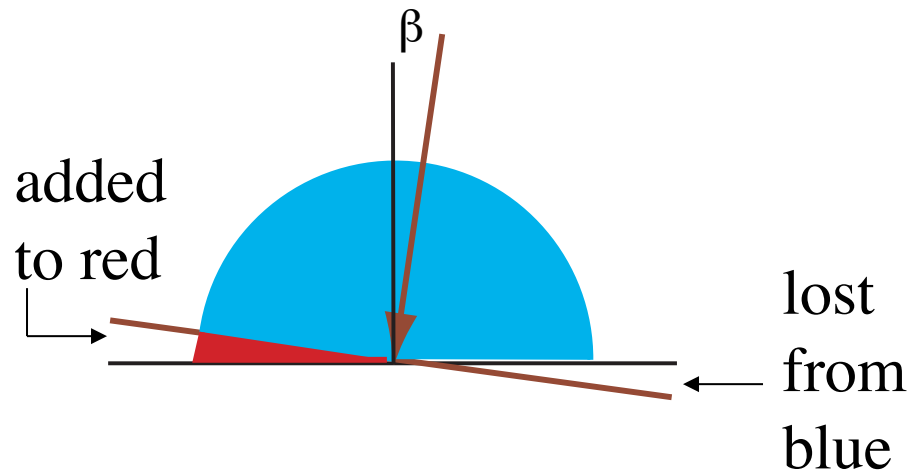

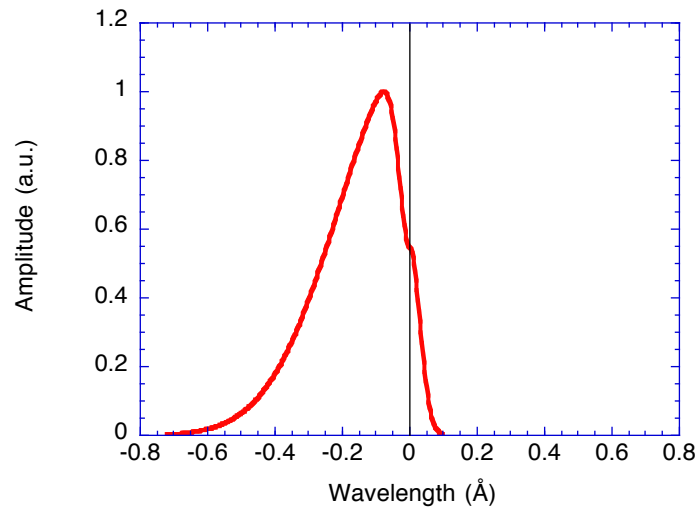

Physical sputtering flux distribution (Thompson)

$$f(E)dE = \frac{E}{(E+U_0)^3}\left[1-\left(\frac{E+U_0}{\gamma(1-\gamma)E_{impact}}\right)^{1/2}\right](\cos\beta)^{\alpha}\,dE$$

Adjustable parameter

$$U_0 = binding\ energy$$

$$\gamma = \frac{4m_1m_2}{(m_1+m_2)^2}$$

No red wing for a perpendicular view !

It is vital to know the rest - wavelength location of the measured spectral line when analyzing data.

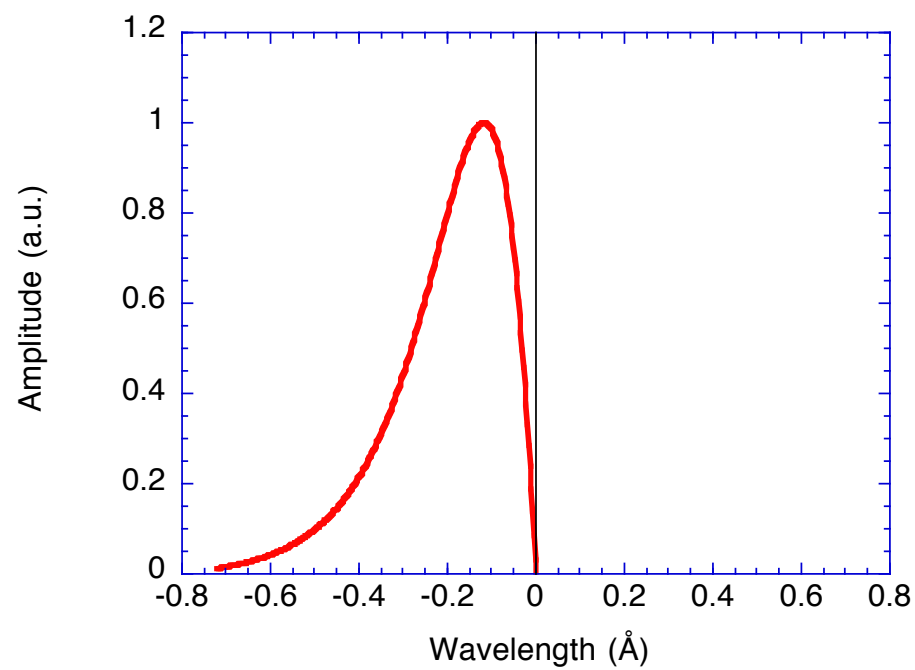

Calculated wavelength distributions

Doppler shift: $\Delta\lambda = \lambda_0 \frac{v}{c} \cos\theta$

By using the Doppler shift relationship, the Thomson flux distribution with a "slow cutoff" and uniform angular distribution is converted to a distribution in $\Delta\lambda$ by integrating over the angles θ and ϕ with appropriate limits.

$$f(\Delta\lambda)d(\Delta\lambda) \propto \int d\varphi \int \left[0.5 m_C \left(\frac{c\,\Delta\lambda}{\lambda_0 \cos\theta}\right)^2 + U_0\right]^{-3} G(\Delta\lambda,\theta)\, \frac{\sin\theta}{\cos^4\theta} (\Delta\lambda)^3\, d\theta\, d(\Delta\lambda)$$

where

$$G(\Delta\lambda,\theta) = 1 - \underbrace{\left[\left(0.5 m_C \left(\frac{c\,\Delta\lambda}{\lambda_0 \cos\theta}\right)^2 + U_0\right) / \gamma(1-\gamma) E_{impact}\right]^{1/2}}_{\text{cutoff term}}$$

and $\gamma = \frac{4 m_D m_C}{(m_D + m_C)^2}$

Requirements for shift measurements

1. Reference line, e.g., Ar I, 9122.967 Å (track 0)

2. Slit image curvature measurements - N. H. Brooks

3. Average dispersion between reference line C I line - N. H. Brooks

4. Accuracy of 0.01-0.02 Å (0.1-0.2 pixel widths)

Line shapes from carbon source experiment - 4/5/00 (Deconvolved profiles)

Inner leg

Ti (major) = 0.55 eV

OSP

E_{impact} = 100 eV

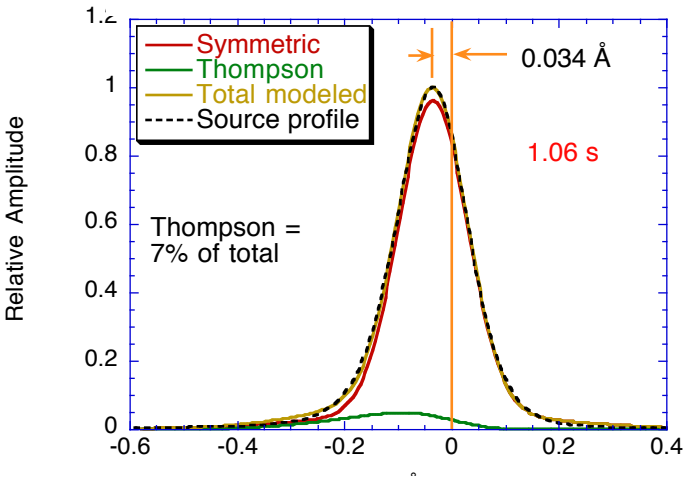

5 MW

E_{impact} = 60 eV

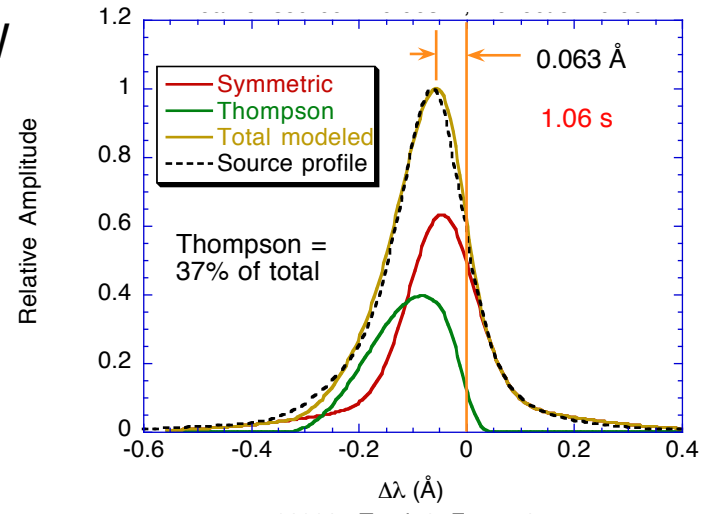

Ti (major) = 0.55 eV

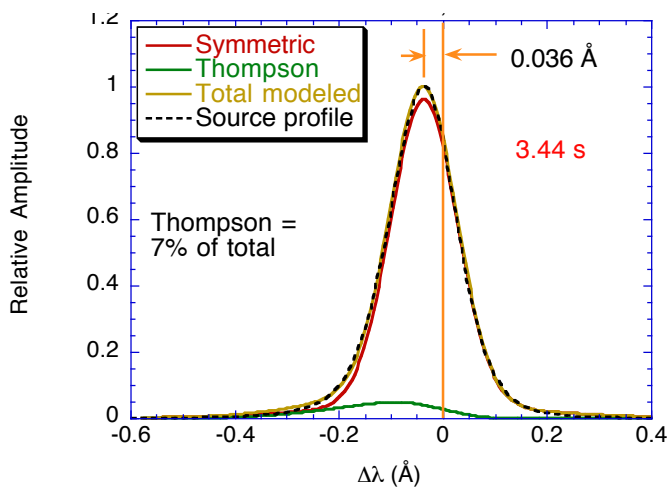

10 MW

E_{impact} = 275 eV

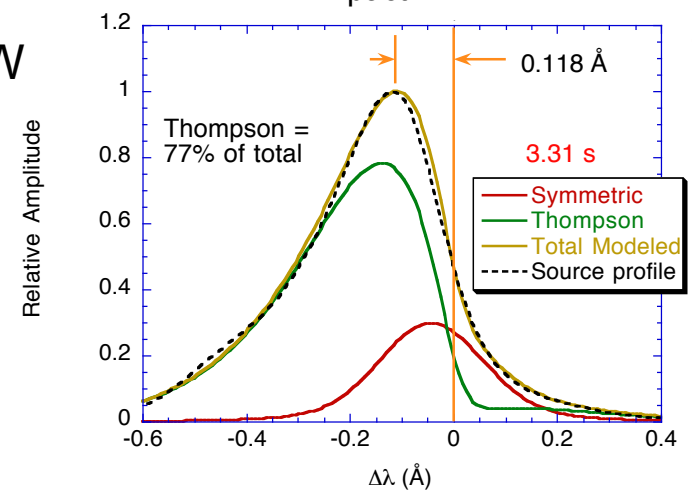

Ti (major) = 1.25 eV

Molecular modeling:CD-PISCES, C_2-DIII-D

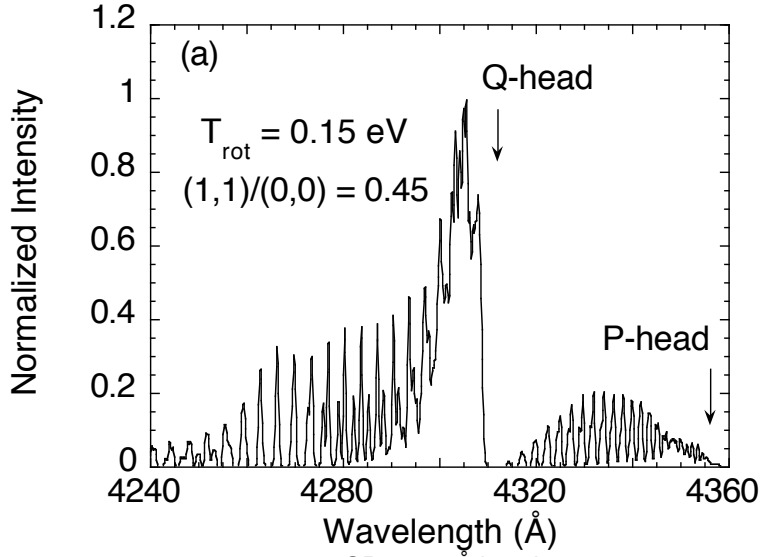

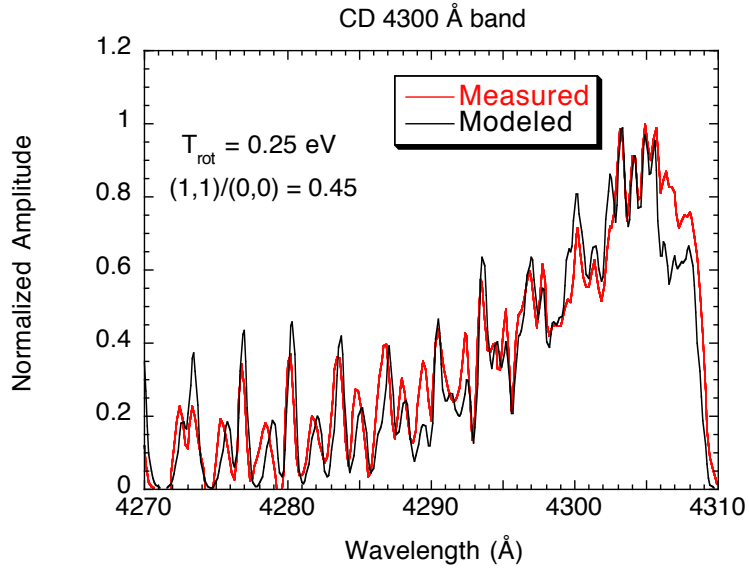

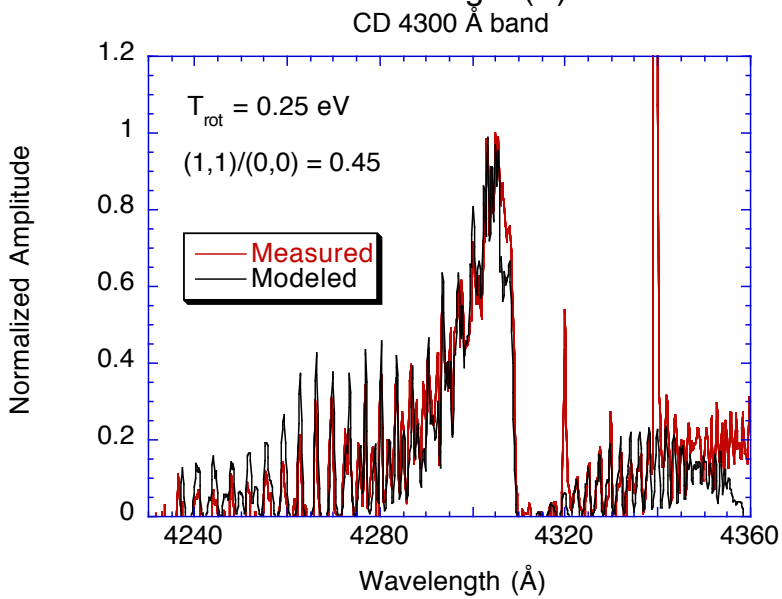

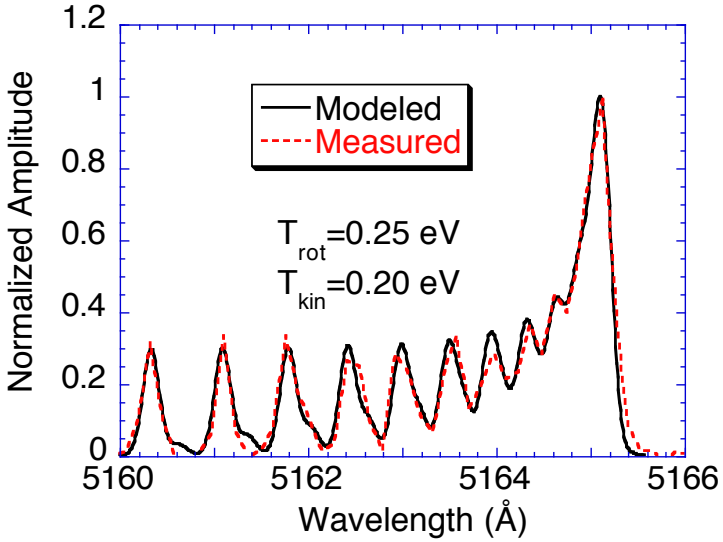

C_2

Finis

Matrix entries for the Stark Effect

$\delta=0^o$

	$S_{1/2}^{-1/2}$	$S_{1/2}^{1/2}$	$P_{1/2}^{-1/2}$	$P_{1/2}^{1/2}$	$P_{3/2}^{-3/2}$	$P_{3/2}^{-1/2}$	$P_{3/2}^{1/2}$	$P_{3/2}^{3/2}$
$S_{1/2}^{-1/2}$	0	0	●	0	0	●	0	0
$S_{1/2}^{1/2}$	0	0	0	●	0	0	●	0
$P_{1/2}^{-1/2}$	●	0	0	0	0	0	0	0
$P_{1/2}^{1/2}$	0	●	0	0	0	0	0	0
$P_{3/2}^{-3/2}$	0	0	0	0	0	0	0	0
$P_{3/2}^{-1/2}$	●	0	0	0	0	0	0	0
$P_{3/2}^{1/2}$	0	●	0	0	0	0	0	0
$P_{3/2}^{3/2}$	0	0	0	0	0	0	0	0

$\delta=90^o$

	$S_{1/2}^{-1/2}$	$S_{1/2}^{1/2}$	$P_{1/2}^{-1/2}$	$P_{1/2}^{1/2}$	$P_{3/2}^{-3/2}$	$P_{3/2}^{-1/2}$	$P_{3/2}^{1/2}$	$P_{3/2}^{3/2}$
$S_{1/2}^{-1/2}$	0	0	0	●	●	0	●	0
$S_{1/2}^{1/2}$	0	0	●	0	0	●	0	●
$P_{1/2}^{-1/2}$	0	●	0	0	0	0	0	0
$P_{1/2}^{1/2}$	●	0	0	0	0	0	0	0
$P_{3/2}^{-3/2}$	●	0	0	0	0	0	0	0
$P_{3/2}^{-1/2}$	0	●	0	0	0	0	0	0
$P_{3/2}^{1/2}$	●	0	0	0	0	0	0	0
$P_{3/2}^{3/2}$	0	●	0	0	0	0	0	0

If δ is between 0° and 90° there will be entries in all positions shown in red